

Adam H. Sobel · J. David Neelin

The boundary layer contribution to intertropical convergence zones in the quasi-equilibrium tropical circulation model framework

Received: date / Accepted: date

Abstract Theories for the position and intensity of precipitation over tropical oceans on climate time scales have a perplexing disagreement between those that focus on the momentum budget of the atmospheric boundary layer (ABL), and those that focus on thermodynamic factors. In the case of narrow intertropical convergence zones (ITCZs), there is some evidence for both classes of theories, and there are large open questions on the interpretation of the moist static energy and momentum budgets of these regions. We develop a model in which both types of mechanisms can operate, and the interaction between them can be analyzed. The model includes a mixed-layer ABL, coupled to a free troposphere whose vertical structure follows the quasi-equilibrium tropical circulation model (QTCM) of Neelin and Zeng. The case analyzed here is axisymmetric, using a fixed sea surface temperature (SST) lower boundary condition with an idealized off-equatorial SST maximum. We examine a regime with small values of the gross moist stability associated with tropospheric motions, which is realistic but poses theoretical challenges. In both rotating (equatorial β -plane) and nonrotating cases, the model ITCZ width and intensity are substantially controlled by horizontal diffusion of moisture, which is hypothesized to be standing in for non-axisymmetric transients. The inclusion of the ABL increases the amplitude and sharpness of the ITCZ, contributing to the importance of diffusion. Analytical solutions under simplifying assumptions show that the ABL contribution is not singular in the nondiffusive limit; it just features an ITCZ more intense than observed. A negative gross moist stability contribution associated with the flow component driven by ABL momentum dynamics plays a large role in this. Because of the ABL contribution, the flow imports, rather than exports, moist static energy in the ITCZ, but we show that this can be understood rather simply. The ABL contribution can be approximately viewed as a forcing to the tropospheric thermodynamics. The ABL forcing term is in addition to thermodynamic forcing by net flux terms in the moist static energy budget, which otherwise is much as in the standard QTCM. The ABL momentum budget suggests that divergent flow in the ABL is controlled to a significant extent by the pressure gradient imprinted on the ABL by the SST gradient—termed the Lindzen–Nigam contribution—although we also find that the thermodynamics mediating this is nontrivial, especially in the rotating case. Nonetheless, when this component of the pressure gradient is artificially removed, the peak ITCZ precipitation is reduced by a fraction on the order of 30-40%, less than might have been expected based on the diagnosis of the ABL momentum budget.

Keywords Atmospheric dynamics · Tropical Meteorology · Moist convection

A. H. Sobel
Columbia University, 500 W. 120th St., Rm. 217, New York, NY 10027
Tel.: +1-212-854-6587
Fax: +1-212-854-8257
E-mail: ahs129@columbia.edu

J. D. Neelin
Dept. of Atmospheric and Oceanic Sciences and Inst. of Geophysics and Planetary Physics, University of California, Los Angeles, 405 Hilgard Ave., Los Angeles, CA 90095-1565

PACS First · Second · More

1 Introduction

Historically, there have been two classes of theories for the quasi-steady (monthly mean) component of tropical precipitation and surface wind, given the sea surface temperature (SST) as a boundary condition. In one, the SST determines the winds directly, through atmospheric boundary layer (ABL) dynamics, and the convergence of the winds at low levels determines the location and intensity of precipitation, essentially through a moisture budget argument. The low-level mass convergence is associated with low-level moisture convergence. This moisture import is assumed to be balanced by moisture loss via precipitation. These theories thus advocate ABL dynamic control of precipitation: ABL momentum dynamics drives deep convection by controlling moisture convergence in the ABL. The studies of Holton (1971), Charney (1971), Lindzen and Nigam (1987), Waliser and Somerville (1994), Tomas and Webster (1997), Tomas et al. (1999), and Pauluis (2004) all belong to this tradition, although they place emphasis on different aspects of ABL momentum dynamics. Some invoke transient disturbances while others consider only steady flow, and some consider only linear dynamics while others involve nonlinear effects. Of these, the study of Lindzen and Nigam (1987; LN hereafter) has had considerable influence. In that theory, the SST determines the atmospheric ABL temperature directly, by turbulent fluxes. Pressure gradients at the top of the ABL are neglected, and surface pressure is determined hydrostatically by the ABL temperature. Given the surface pressure field, a linear momentum balance determines the winds, and the convergence of the winds determines precipitation via the moisture budget as described above. This theory is appealing because of its simplicity, apparently by-passing the complications of moist and radiative physics. The ABL momentum budget unambiguously comes first, and determines the precipitation. The precipitation, and its associated convective heating, need not be known in order to determine the surface wind. Because the surface fluxes are implicitly assumed to tie ABL temperature to SST so strongly that other thermodynamics factors are irrelevant, how the energy budget is balanced is not a consideration in this theory.

In another historical class of theories, precipitation is determined by SST and related factors such as the temperature and moisture vertical profile and surface and radiative fluxes. These may be loosely lumped as assuming a leading role for thermodynamics in the control of precipitation. In some of these theories the precipitation tends to be determined by the local SST and its effects on local profiles of temperature and humidity. The surface winds are induced by the heating associated with the precipitation and may feed back on the thermodynamic fields. Many “first baroclinic mode” models, containing a single vertical degree of freedom and no ABL (e.g., Matsuno 1966; Webster 1972, 1980; Gill 1980; Zebiak 1982, 1986; Davey and Gill 1987; Weare 1987; Seager 1991; Kleeman 1991), fall roughly into this class. Such models tend to have trouble simulating ITCZs as narrow and intense as observed (e.g., Seager 1991; Kleeman 1991). Thermodynamic control is particularly clear when the “weak temperature gradient” approximation is used (Neelin and Held 1987; Zeng and Neelin 1999; Sobel and Bretherton, 2000). These assume that horizontal deep baroclinic wave speeds are fast relative to other time scales, such that tropospheric temperature is approximately uniform. Vertical motion, convergence and precipitation are determined by the moist thermodynamics, such as the moist static energy budget (Neelin and Held 1987; Neelin 1997; Raymond 2000). Other such theories consider free-tropospheric humidity (Raymond 2000), convective inhibition (CIN; Mapes 2000), or a combination thereof (Raymond et al., 2003).

The two classes of theories appear fundamentally different. In one, the boundary layer momentum budget determines winds, hence convergence; in the other, thermodynamic considerations determine convergence, hence winds. In both, precipitation is typically diagnostic from moisture convergence. At a gross level, both predict that rainfall will maximize near SST maxima, so distinguishing between them requires looking at features finer than this. The LN model can be mapped mathematically onto simple models of the thermodynamic control class (Neelin 1988), so being able to distinguish them depends on specifics of physics and parameter values. While small-scale convection itself must depend on buoyancy available to convective plumes, essentially a thermodynamic effect, this is not where the theories diverge. The disagreement comes in how best to short cut to the large scale controls on the convection. Part of this difference in approaches comes from time scales associated with diabatic fluxes versus wave dynamical time scales associated with stratification in the troposphere. As noted in Neelin

(1997) and Yu and Neelin (1997), the tropical tropospheric circulation is a compromise between (i) surface and radiative fluxes plus fast deep convective time scales, which tend to draw the troposphere toward a state with warmer tropospheric temperatures over warmer SST; and (ii) fast horizontal baroclinic wave time scales, which oppose this, smoothing the pressure gradients. If the first process dominated, as in a thermal circulation argument or the LN model in the ABL, it would control the tropospheric circulation dynamically via these pressure gradients. If the latter dominates, as in the WTG limit, one obtains the thermodynamic control case. The troposphere leans toward the latter by virtue of the fast wave speeds, while the ABL tends to the former.

More recently, there have been theoretical developments based on working out the implications of convective quasi-equilibrium (QE) (Arakawa and Schubert 1974; Emanuel et al 1994) for tropospheric dynamics interacting with deep convection. Convective QE posits that buoyancy available to convecting elements tends to be removed quickly, bringing moisture and temperature in each column toward a statistical equilibrium in vertical structures. An approach that constructs primitive equation models by Galerkin projection on vertical basis functions derived from asymptotic solutions under convective QE was presented in Neelin and Zeng (2000, NZ hereafter). Termed quasi-equilibrium tropical circulation models (QTCMs), these are truncated to few vertical degrees of freedom, whose structures are tailored to the physics of the problem. They are thus intermediate complexity climate models. The initial version, QTCM1, has a single baroclinic degree of freedom, plus a barotropic mode, and thus has aspects in common with earlier idealized models. It differs by retaining full primitive equation nonlinearity, consistent moisture and energy budgets, and incorporating a set of physical parameterizations designed to be close in behavior to those used in more complex general circulation models (GCMs).

The NZ approach permits simulation of a number of things that are not easily asked of ABL dynamic control theory, such as the climatology and interannual anomalies of precipitation over land as well as ocean (Zeng et al. 2000); surface and top of atmosphere net energy fluxes; remote ENSO impacts mediated by moist wave dynamics (Su and Neelin 2002; Neelin and Su 2005); phase lags associated with atmosphere-ocean surface layer adjustment (Su et al 2005); impacts of midlatitude variability on tropical variance (Lin et al 2000; Su and Neelin 2003); modern and paleo theory of land monsoons (Chou and Neelin 2003; Su and Neelin 2005) and tropical precipitation changes under global warming (e.g., Neelin et al 2003; Chou and Neelin 2004). When forced with realistic geography, SST distributions, insolation, and land surface boundary conditions, QTCM1 tends to simulate such features in a manner comparable to that of coarse resolution GCMs.

However, this approach was never intended to exclude contributions by the LN mechanism or other ABL effects. Indeed the QTCM framework aims to permit additions of such contributions. The basis function choice in QTCM1 reflects a deep tropospheric temperature structure with associated baroclinic wind structures because these are leading contributors in response to deep convection, radiation, and the flow field of the general circulation. This permits a simulation of many climate features, but it is known that addition of a passive boundary layer for wind turning (Stevens et al 2002) modifies the surface stress, and that addition of a second vertical degree of freedom in moisture can have quantitative impacts on the ITCZs and transient phenomena such as dry intrusions (Neggers et al 2005a). There are a number of reasons to believe that in regions of sharp SST gradients an LN contribution is likely (Wang and Li 1993; Chiang et al. 2001). GCM and reanalysis diagnostics by Bacmeister and Suarez (2002) suggest that while the LN contribution to low level pressure gradients is often small relative to free tropospheric contributions, in the eastern Pacific ITCZ the LN contribution (to the zonal component of the wind; they did not consider the meridional) may be significant.

We here construct a model with QTCM1 as a starting point, but with added degrees of freedom to represent ABL dynamics explicitly. This permits examination of the interplay between thermodynamic and ABL dynamic mechanisms in a relatively tractable model that contains both. The aim is to identify aspects of the ITCZ response associated with flow driven by ABL temperature gradients, termed the LN contribution, and aspects that yield an ITCZ in the original NZ QTCM, which we term for brevity the NZ contribution. The model is implemented here in an axisymmetric case because this is anticipated to have a significant LN contribution.

While an idealized case of the model is presented to address a particular set of questions, we anticipate that the formulation will be incorporated into a full QTCM climate model in future. Such a model, with two baroclinic degrees of freedom associated with the free troposphere and ABL (plus a barotropic mode), will be termed QTCM2. The equations, aside from the simplified physical parameterizations used here, provide a prototype for those that will constitute QTCM2.

Besides addressing the relative role of the LN and NZ contributions to ITCZ rainfall, the set-up here can shed light on a long-standing but lesser known question. The moist static energy budget of convection zones contains large cancellation between import of moisture and export of dry static energy. This can make estimation of the mean flow net moist static energy (MSE) transport difficult, and has left open questions regarding the degree of cancellation, the representation of this as an effective moist stability and the relative contribution of MSE export by transients and the mean flow (Oort 1983; Neelin and Held 1987; Trenberth and Solomon 1994; Yu et al 1998). L. Back and C. Bretherton (personal comm. 2005) recently find that in some reanalysis data sets, the mean flow tends to have small mean export or even import MSE in regions of narrow sharp ITCZs. In the model here, this apparent oddity, that would seem to imply a thermodynamically indirect mean flow, is easily resolved by breaking out the transport associated with the ABL.

2 Model

2.1 Primitive equations

The horizontal velocity, \mathbf{v} , whose components in the x and y directions are u and v pressure vertical velocity ω ; temperature T in energy units, i.e., temperature in Kelvin multiplied by c_p the heat capacity of air at constant pressure; and specific humidity q in energy units, i.e., specific humidity in kg/kg multiplied by the latent heat of vaporization satisfy the primitive equations in pressure coordinates:

$$\frac{d\mathbf{v}}{dt} + \omega\partial_p\mathbf{v} + f\mathbf{k} \times \mathbf{v} = -\nabla\phi + \mathbf{F}, \quad (1)$$

$$\frac{dT}{dt} + \omega\partial_p s = Q_c + Q_R, \quad (2)$$

$$\frac{dq}{dt} + \omega\partial_p q = Q_q, \quad (3)$$

$$\nabla \cdot \mathbf{v} + \partial_p\omega = 0, \quad (4)$$

where f is the Coriolis parameter, ϕ the geopotential, \mathbf{F} any frictional force, ω pressure vertical velocity, Q_c convective heat source and Q_q convective moisture sink (e.g., Yanai et al. 1973), and Q_R radiative heating. Here $d/dt = \partial_t + \mathbf{v} \cdot \nabla$, the total derivative following the horizontal component of the motion, and $\nabla \cdot \mathbf{v}$ is the horizontal divergence.

2.2 Vertical structure

We assume that \mathbf{v} , T , and q above the ABL are represented by a small number of vertical structures:

$$\mathbf{v}(x, y, p, t) = V_0(p)\mathbf{v}_0(x, y, t) + V_1(p)\mathbf{v}_1(x, y, t) \quad (5)$$

$$T(x, y, p, t) = T_r(p) + a_1(p)T_1(x, y, t) \quad (6)$$

$$q(x, y, p, t) = q_r(p) + b_1(p)q_1(x, y, t), \quad (7)$$

as in QTCM1. In that model, these structures were defined for the entire vertical model domain, $p_t < p < p_s$ where p_t is the nominal tropopause pressure and p_s is the reference surface pressure.

The constant profiles T_r and q_r are separated out because variations in T , q are often small compared to their mean values. The perturbation structure function for temperature $a_1(p)$, is constructed from observations in the tropical atmosphere, and is close to a moist adiabat. The profile for baroclinic velocity, $V_1(p)$, is constructed to be consistent with a_1 , assuming that the pressure gradient force obtained from a_1 by hydrostatic balance has the same vertical structure as the other linear terms in the momentum equation.

Here, our approach is to “lift the bottom” of the original QTCM, and place a mixed layer representation of the ABL under it. That is, the free troposphere will be represented by vertical basis functions which are the same as those used for the entire troposphere in the QTCM (NZ; Zeng et al. 2000), but the new model’s modes will be defined starting at the top of the ABL instead of at the surface. Thus, (5)-(7) now describe the vertical structures for for $p_t < p < p_e$, where p_e is the top of the ABL, with a_1 , b_1 , V_1 , and V_0 all zero in the ABL.

ABL vertical structures are taken to be constant within the ABL (zero above) for \mathbf{v} , q and dry static energy s . Thus between surface and ABL top, i.e., for $p_s > p > p_e$,

$$\mathbf{v}(x, y, p, t) = \mathbf{v}_b(x, y, t) \quad (8)$$

$$s(x, y, p, t) = s_{rb} + s_b(x, y, t) \quad (9)$$

$$q(x, y, p, t) = q_{rb} + q_b(x, y, t), \quad (10)$$

where s_{rb} and q_{rb} are reference values for ABL dry static energy and specific humidity. The ABL temperature structure a_b , required for computing pressure gradients, is simply given by the dry adiabat using s_b .

$$T(x, y, p, t) = T_r(p) + a_b(p)s_b(x, y, t), \quad p_e < p < p_s \quad (11)$$

with the reference profile T_r within the ABL consistent with s_r . For the purpose of defining the vertical mode structures, we neglect variations in both p_s and p_e . Neglecting variations in the pressure of the ABL top, p_e , means that the ABL top is not defined as a Lagrangian surface, as is typically done in ABL modeling (e.g., see Stevens, this volume). Our model is better thought of as being projected on a set of basis functions which are divided into two subsets occupying different pressure ranges.

The vertical velocity structure function $\Omega_1(p)$ is obtained from V_1 as in NZ, consistent with mass conservation (4):

$$\Omega_1(p) = \int_{p_t}^p V_1(\hat{p})d\hat{p}, \quad p_t < p < p_e; \quad 0 \text{ otherwise.} \quad (12)$$

There is now a choice to make regarding V_1 that affects the partition of mass and momentum conservation among basis functions. We choose V_1 such that its vertical integral over the free troposphere is zero. This has the useful property that the free-tropospheric barotropic and baroclinic basis functions are, as in QTCM1, orthogonal:

$$\int_{p_t}^{p_e} V_1(p)V_0(p)dp = 0. \quad (13)$$

This also implies in (12) that Ω_1 goes to zero at p_e (rather than at p_s in NZ). Thus all mass convergence (divergence) in the ABL must be balanced by divergence (convergence) in the ‘‘barotropic’’ free tropospheric component.

$$p_B \nabla \cdot \mathbf{v}_b = -p_F \nabla \cdot \mathbf{v}_0 = \omega_e, \quad (14)$$

where the depths of the ABL and free troposphere are

$$p_B = p_s - p_e, \text{ and } p_F = p_e - p_t, \quad (15)$$

and ω_e is the vertical velocity at ABL top. We use a rigid lid upper boundary condition $\omega = 0$ at the tropopause p_t , and $\omega = 0$ at the surface, neglecting terms such as $\mathbf{v} \cdot \nabla p_s$. This does not require us to hold the surface geopotential constant; we can diagnose changes in that quantity from the momentum equations, as discussed below. Note that the rotational mass transport in the ABL and free-tropospheric barotropic mode need not be equal and opposite.

The vertical velocity structure Ω_0 is found by integrating mass continuity (4) for ABL and V_0 basis functions separately, and using (14)

$$\Omega_0 = p - p_t, \quad p_t < p \leq p_e, \quad (16)$$

$$= (p_s - p)(p_F/p_B), \quad p_e < p \leq p_s. \quad (17)$$

The total vertical velocity is thus

$$\omega(x, y, p, t) = -\Omega_0 \nabla \cdot \mathbf{v}_0 - \Omega_1 \nabla \cdot \mathbf{v}_1, \quad (18)$$

where negative ω is upward, Ω_i are defined positive, and $\nabla \cdot \mathbf{v}_1$, $\nabla \cdot \mathbf{v}_0$ are positive for divergence in the upper troposphere.

These vertical structures are not modes in the sense of normal modes, although because V_1 , Ω_1 and a_1 are chosen to be consistent under certain approximations in the primitive equations, it is convenient to refer to these as the baroclinic mode, and to \mathbf{v}_0 as the barotropic mode. If the model is linearized about a barotropic mean state and damping and heating terms are neglected, there is a nondivergent barotropic mode consisting of \mathbf{v}_0 and an equal \mathbf{v}_b . The first baroclinic mode under these circumstances has \mathbf{v}_1 , T_1 components along with \mathbf{v}_b and \mathbf{v}_0 contributions that make its vertical velocity look much like that of QTCM1. When vertical drag terms and rotation are included, the alterations are nontrivial due to ABL Ekman pumping (Moskowitz and Bretherton, 2000).

2.3 Model equations in flux form

For the free troposphere, we assume the vertical structures described above and perform vertical integrations to obtain the model equations, essentially a low-order Galerkin truncation. The model temperature, moisture, and barotropic momentum equations are obtained by vertical averaging of the respective three-dimensional equations for those variables, while the baroclinic equation is obtained by first multiplying the momentum equation by $V_1(p)$ and then averaging. We obtain the flux-form equations for free-tropospheric temperature:

$$\begin{aligned} \hat{a}_1[\partial_t T_1 + \nabla \cdot (\mathbf{v}_0 T_1)] + \hat{s}_r \nabla \cdot \mathbf{v}_0 + \langle V_1 a_1 \rangle^F \nabla \cdot (\mathbf{v}_1 T_1) + \langle V_1 s_r \rangle^F \nabla \cdot \mathbf{v}_1 + \left(\frac{p_B}{p_F}\right) s^\dagger \nabla \cdot \mathbf{v}_b \\ = \langle Q_c \rangle^F + \langle Q_R \rangle^F + (s_b - s_e) \tau_m^{-1}, \end{aligned} \quad (19)$$

moisture,

$$\begin{aligned} \hat{b}_1[\partial_t q_1 + \nabla \cdot (\mathbf{v}_0 q_1)] + \hat{q}_r \nabla \cdot \mathbf{v}_0 + \langle V_1 b_1 \rangle^F \nabla \cdot (\mathbf{v}_1 q_1) + \langle V_1 q_r \rangle^F \nabla \cdot \mathbf{v}_1 + \left(\frac{p_B}{p_F}\right) q^\dagger \nabla \cdot \mathbf{v}_b \\ = \langle Q_q \rangle^F + (q_b - q_e) \tau_m^{-1} + k_q \nabla^2 q_1, \end{aligned} \quad (20)$$

barotropic velocity,

$$\partial_t \mathbf{v}_0 + \nabla \cdot (\mathbf{v}_0 \mathbf{v}_0) + \langle V_1^2 \rangle^F \nabla \cdot (\mathbf{v}_1 \mathbf{v}_1) + \left(\frac{p_B}{p_F}\right) \mathbf{v}^\dagger \nabla \cdot \mathbf{v}_b + f \hat{\mathbf{k}} \times \mathbf{v}_0 = -\nabla (\kappa a_b^{+e} s_b + \kappa \langle a_1^+ \rangle^F T_1 + \phi_s) + (\mathbf{v}_b - \mathbf{v}_e) \tau_m^{-1}, \quad (21)$$

where $\hat{\mathbf{k}}$ is the vertical unit vector, and baroclinic velocity,

$$\partial_t \mathbf{v}_1 + \nabla \cdot (\mathbf{v}_0 \mathbf{v}_1) + \langle V_1^3 \rangle^F / \langle V_1^2 \rangle^F \nabla \cdot (\mathbf{v}_1 \mathbf{v}_1) + \left(\frac{p_B}{p_F}\right) V_{1e} \mathbf{v}^\dagger \nabla \cdot \mathbf{v}_b + f \hat{\mathbf{k}} \times \mathbf{v}_1 = -\kappa \nabla T_1 - \epsilon_1 \mathbf{v}_1 + V_{1e} (\mathbf{v}_b - \mathbf{v}_e) \tau_m^{-1} + \hat{\mathbf{j}} k_v \nabla^2 v_1 \quad (22)$$

In the above, we have defined the average over the free troposphere

$$\langle x \rangle^F = \hat{x} = p_F^{-1} \int_{p_t}^{p_e} x \, dp,$$

\mathbf{v}_e, s_e, q_e , refer to total values just above ABL top, e.g.,

$$s_e = s_{re} + a_1(p_e) T_1,$$

and we have introduced the notational shorthand $V_{1e} \equiv V_1(p_e)$. We allow for the possibility that the reference profiles for dry static energy and specific humidity do not match at the ABL top, so s_{re} is the dry static energy computed from T_r at a pressure infinitesimally less than p_e .

Equation (14), has been used in deriving the above, resulting in the terms in $\nabla \cdot \mathbf{v}_b$, with $\mathbf{v}^\dagger, s^\dagger, q^\dagger$ values just above ABL top, used to calculate the vertical advection across the boundary layer top as discussed further below. The coefficients a_b^{+e} and $\langle a_1^+ \rangle^F$ come from integrating temperature to obtain geopotential using hydrostatic balance and are defined explicitly below. Horizontal diffusivity coefficients are k_q for moisture and k_v for meridional velocity, with $\hat{\mathbf{j}}$ the unit vector in the y direction. No horizontal diffusion is applied to zonal velocity or temperature.

The surface geopotential ϕ_s appears in (21) along with baroclinic geopotential contributions to the vertical average from both T_1 and s_b . The presence of these three pressure gradient terms is a consequence of using the surface as the reference level in integrating the hydrostatic equation. The ABL momentum equation (below) has two. The right hand side of (22) has only one pressure gradient term in it, proportional to ∇T_1 . This is a consequence of our choice to keep $\Omega_1 = 0$ at p_e , analogously to the QTCM treatment of that mode at the surface.

For the boundary layer, the procedure is essentially the same, but simpler, as each variable has only one mode, and each prognostic variable q, s, \mathbf{v} is assumed uniform in height. We thus obtain the equations for ABL dry static energy,

$$\partial_t s_b + \nabla \cdot [\mathbf{v}_b (s_{rb} + s_b)] - s^\dagger \nabla \cdot \mathbf{v}_b = \frac{g}{p_B} H + \langle R \rangle^b + \langle Q_c \rangle^b - \frac{p_F}{p_B} (s_b - s_e) \tau_m^{-1} + k_q \nabla^2 s_b, \quad (23)$$

specific humidity,

$$\partial_t q_b + \nabla \cdot [\mathbf{v}_b (q_{rb} + q_b)] - q^\dagger \nabla \cdot \mathbf{v}_b = \frac{g}{p_B} E + \langle Q_q \rangle^b - \frac{p_F}{p_B} (q_b - q_e) \tau_m^{-1} + k_q \nabla^2 q_b \quad (24)$$

and velocity,

$$\partial_t \mathbf{v}_b + \nabla \cdot (\mathbf{v}_b \mathbf{v}_b) - \mathbf{v}^\dagger \nabla \cdot \mathbf{v}_b = -\nabla(\kappa \langle a_b^+ \rangle^b s_b + \phi_s) - \epsilon_b \mathbf{v}_b - \frac{p_F}{p_B} (\mathbf{v}_b - \mathbf{v}_e) \tau_m^{-1} + \hat{\mathbf{j}} k_v \nabla^2 v_b. \quad (25)$$

E and H are the surface fluxes of latent and sensible heat, respectively, and we have defined the vertical average over the boundary layer,

$$\langle x \rangle^b = p_B^{-1} \int_{p_e}^{p_s} x dp. \quad (26)$$

The coefficient of the baroclinic ABL geopotential contribution $\langle a_b^+ \rangle^b$ is defined below. Terms like $x^\dagger \nabla \cdot \mathbf{v}_b$, where x is s , q , or \mathbf{v} , are vertical advective fluxes. In computing these terms, the constancy of p_s and p_t has been used, as has mass conservation. \mathbf{v}^\dagger , s^\dagger , q^\dagger are the values used to compute the vertical advective fluxes. Here we use two possible formulations for these values. The ‘‘upwind’’ formulation is, using dry static energy as an example,

$$\begin{aligned} s^\dagger &= s_{rb} + s_b \quad \text{if } \nabla \cdot \mathbf{v}_b < 0, \\ s^\dagger &= s_e \quad \text{if } \nabla \cdot \mathbf{v}_b > 0, \end{aligned}$$

The ‘‘centered’’ formulation is

$$s^\dagger = \frac{1}{2} (s_{rb} + s_b + s_e). \quad (27)$$

The upwind formulation implies that upward motion (occurring mostly in convective regions) does not affect the ABL, while subsidence does. The centered formulation has the advantage that it can be linearized about zero vertical velocity, for example to study the properties of linear waves in the model. In the appendix we briefly describe the sensitivity of nonlinear simulations to the choice of vertical advection scheme.

The terms in τ_m^{-1} are meant to represent turbulent exchange between the free troposphere and the ABL other than that explicitly represented by the deep convective parameterization. It can be viewed as representing dry turbulent entrainment as well as a very crude parameterization of shallow moist convection. In the simulations presented in the body of the paper, we allow it to remain active at all times, including when deep convection is on. In reality, deep convection tends to be intermittent, with shallow convection occurring in its absence. Thus it is reasonable to allow both processes to be active in the ensemble average represented here. We have also performed simulations with a version in which the τ_m^{-1} terms in temperature and moisture equations are multiplied by $[1 - \mathcal{H}(Q_c)]$, where $\mathcal{H}(Q_c)$ is the Heaviside function, such that they vanish when deep convection is active. Impacts are briefly discussed in the appendix.

The pressure gradient term in the original 3D momentum equation is $\nabla(\int_p^{p_s} T d \ln p + \phi_s)$. The pressure gradient terms which appear in the different momentum equations then have coefficients which arise from vertical integration:

$$a_b^{+e} = \int_{p_e}^{p_s} a_b d \ln p = a_b^+(p_e), \quad (28)$$

$$\langle a_b^+ \rangle^b = p_B^{-1} \int_{p_e}^{p_s} \int_p^{p_s} a_b d \ln p dp. \quad (29)$$

$$(30)$$

The momentum equations also involve the gradient of the surface geopotential, ϕ_s . This can be found by taking the divergence of (21), since \mathbf{v}_0 itself is already known from (14), once \mathbf{v}_b is. In the implementation here we neglect the tendency term in (21). Also, in this axisymmetric version of the model, it is not necessary to take the divergence. The y -component of (21) in the axisymmetric case is, dropping the tendency term,

$$\partial_y(v_0 v_0) + \langle V_1^2 \rangle^F \partial_y(v_1 v_1) + \frac{p_B}{p_F} v^\dagger \partial_y v_b + f u_0 = -\partial_y(\kappa a_b^{+e} s_b + \kappa \langle a_1^+ \rangle^F T_1 + \phi_s) + (v_b - v_e) \tau_m^{-1}. \quad (31)$$

All quantities in (31) besides ϕ_s are known if the other dependent model variables are, so the equation can be solved diagnostically for $\partial_y \phi_s$, which is needed to solve the y -component of the ABL momentum equation (25).

2.4 Advective form and gross moist stability

Writing the free tropospheric thermodynamic equations in advective form introduces the gross moist stability, a diagnostic which has been found to be useful in a variety of contexts. The flux form can be transformed into the advective by using integration by parts. Terms involving integrals of the velocity basis functions V_i , where i here is 1 or 0, obey

$$\langle V_i x \rangle^F = p_F^{-1} [(\Omega_i x)_{p_t} - (\Omega_i x)_{p_e}] - \langle \Omega_i \partial_p x \rangle,$$

where x is a_1, b_1, s_r , or q_r and the Ω_i are the vertical velocity basis functions,

$$\Omega_i = \int_{p_t}^p V_i dp.$$

Using this the free tropospheric temperature and moisture equations become

$$\begin{aligned} \hat{a}_1 [\partial_t T_1 + \mathbf{v}_0 \cdot \nabla T_1] + M_{s0} \nabla \cdot \mathbf{v}_0 + \langle V_1 a_1 \rangle^F \mathbf{v}_1 \cdot \nabla T_1 + M_{s1} \nabla \cdot \mathbf{v}_1 + \left(\frac{p_B}{p_F}\right) (s^\dagger - s_e) \nabla \cdot \mathbf{v}_b \\ = \langle Q_c \rangle^F + \langle Q_R \rangle^F + (s_b - s_e) \tau_m^{-1}, \end{aligned} \quad (32)$$

$$\begin{aligned} \hat{b}_1 [\partial_t q_1 + \mathbf{v}_0 \cdot \nabla q_1] - M_{q0} \nabla \cdot \mathbf{v}_0 + \langle V_1 b_1 \rangle^F \mathbf{v}_1 \cdot \nabla q_1 - M_{q1} \nabla \cdot \mathbf{v}_1 + \left(\frac{p_B}{p_F}\right) (q^\dagger - q_e) \nabla \cdot \mathbf{v}_b \\ = \langle Q_q \rangle^F + (q_b - q_e) \tau_m^{-1} + k_q \nabla^2 q_1, \end{aligned} \quad (33)$$

where we have defined the gross dry static stabilities and gross moisture stratifications:

$$M_{si} = M_{sri} + M_{spi} T_1 = -\langle \Omega_i \partial_p s_r \rangle^F - \langle \Omega_i \partial_p a_1 \rangle^F T_1, \quad (34)$$

$$M_{qi} = M_{qri} + M_{qpi} q_1 = \langle \Omega_i \partial_p q_r \rangle^F + \langle \Omega_i \partial_p b_1 \rangle^F q_1. \quad (35)$$

Notice also the changes in the terms in $\nabla \cdot \mathbf{v}_b$ from (19) and (20) to (32) and (33); these are due to the boundary terms in the integration by parts of the barotropic divergence terms. The baroclinic terms introduce no such boundary terms as Ω_1 vanishes at p_e and p_t .

The gross moist stability appears in the free tropospheric moist static energy equation, derived by adding (32) and (33):

$$\begin{aligned} [\partial_t + \mathbf{v}_0 \cdot \nabla] h_1 + M_0 \nabla \cdot \mathbf{v}_0 + \mathbf{v}_1 \cdot \nabla (\langle V_1 a_1 \rangle^F T_1 + \langle V_1 b_1 \rangle^F q_1) + M_1 \nabla \cdot \mathbf{v}_1 + \left(\frac{p_B}{p_F}\right) (h^\dagger - h_e) \nabla \cdot \mathbf{v}_b \\ = \langle Q_c \rangle^F + \langle Q_q \rangle^F + \langle Q_R \rangle^F + (h_b - h_e) \tau_m^{-1}, \end{aligned} \quad (36)$$

where $h_1 = \langle a_1 \rangle^F T_1 + \langle b_1 \rangle^F q_1$, $h_b = s_b + q_b$, $h^\dagger = s^\dagger + q^\dagger$, $h_e = s_e + q_e$, and we have defined the gross moist stabilities

$$M_0 = M_{s0} - M_{q0}, \quad (37)$$

$$M_1 = M_{s1} - M_{q1}. \quad (38)$$

In our implementation of the model here, we solve the free tropospheric equations in advective form. Because we wish to consider the gross moist stability as a diagnostic, it makes sense to integrate equations in which this quantity explicitly appears. We solve the ABL equations in flux form.

To produce a moist static energy budget for the entire troposphere, we add p_F times (36), p_B times (23), and p_B times (24) to obtain

$$\begin{aligned} \partial_t (p_F h_1 + p_B h_b) + \mathbf{v}_0 \cdot \nabla h_1 + \mathbf{v}_b \cdot \nabla h_b + p_F \mathbf{v}_1 \cdot \nabla (\langle V_1 a_1 \rangle^F T_1 + \langle V_1 b_1 \rangle^F q_1) + p_F M_1 \nabla \cdot \mathbf{v}_1 \\ - p_B M_B \nabla \cdot \mathbf{v}_b = g F^{\text{net}}, \end{aligned} \quad (39)$$

where $h_b = s_b + q_b$, and we have used (14) repeatedly. In the above, notice that all terms in s^\dagger, q^\dagger , with their associated ‘‘if’’ statements (if the upwind scheme is used), have vanished, as have terms in τ_m^{-1} . All convective heating and moistening terms have also vanished, due to energy conservation [see equation (54), below].

We have defined

$$M_B = (h_b - h_e) - M_0 \quad (40)$$

as the gross moist stability experienced by rising motions from the ABL through the entire ABL and troposphere. Note that this is equivalent to $\langle \Omega_0 \partial_p h \rangle$. The part M_0 associated with motion through the troposphere, is needed separately in (36) because of the vertical advection terms.

The diabatic driving of the equation is by the net vertical flux of radiative, sensible and latent heat fluxes into the column at top and bottom of the atmosphere

$$F^{\text{net}} = E + H + (p_F/g)\langle Q_R \rangle^F + (p_B/g)\langle Q_R \rangle^b \quad (41)$$

noting that the Q_R heating terms are vertical divergences of radiative fluxes.

Parameters used in the runs here are given in Table 1, including the contributions to the tropospheric and ABL gross moist stability. Because the moisture field tends to adjust quite strongly to the flow, especially in convective regions, the reference value for moisture is not a good indicator of the moisture contribution to M_1 , that is, the second term on the RHS of (35) is generally important. Gross moist stability properties are best diagnosed from the simulations.

3 Physics

3.1 Surface fluxes

Surface fluxes are parameterized by standard bulk formulae, with the dependence on surface wind speed neglected:

$$E = \rho_a C_D V_s (q^*(T_s) - q_b) \quad (42)$$

$$H = \rho_a C_D V_s (T_s - s_b) \quad (43)$$

where $q^*(T_s)$ is the saturation specific humidity at the SST, T_s , C_D is the exchange coefficient, ρ_a is the surface air density, and V_s is the surface wind speed. In general V_s should depend on $|\mathbf{v}_b|$ plus a parameterization of contributions by non-resolved variance, but here we set V_s to a constant. This is a strong simplification, but we make it because we are interested in steady solutions and under some circumstances wind-dependent surface fluxes can lead to the growth of time-dependent disturbances due to wind-evaporation feedbacks or ‘‘WISHE’’ (Emanuel 1987; Neelin et al. 1987). For later use, we define a characteristic time scale over which surface fluxes act on the ABL:

$$\tau_s^{-1} = \frac{g}{p_B} \rho_a C_D V_s. \quad (44)$$

3.2 Radiation

Radiation is here parameterized more simply than in a full QTCM. In the free troposphere, we use a Newtonian cooling:

$$\langle Q_R \rangle^F = \frac{T_R - T_1}{\tau_R} \quad (45)$$

where T_R is a radiative equilibrium temperature (relative to the reference temperature T_r) and τ_R a radiative time scale. In the boundary layer, we use the scheme:

$$\langle Q_R \rangle^b = Q_{Rb0} + \frac{T_s - s_{rb} - s_b}{\tau_{Rb}} \quad (46)$$

where Q_{Rb0} is a negative constant and τ_{Rb} is the time scale on which the boundary layer is relaxed towards the SST by radiative processes alone, estimated from linearization of a grey-body scheme. This scheme is admittedly quite crude, but for appropriate values of Q_{Rb0} and τ_{Rb} it at least has the desirable result of making sure that the ABL temperature stays close to the SST, as observed, while still the total radiative heating of the ABL is negative.

3.3 Convective Closure

As in the standard QTCM, we start from the Betts-Miller convective scheme (Betts 1986; Betts and Miller 1986), project it on the assumed vertical structures, and make some additional simplifications. Here, however, the result differs materially from the standard QTCM because of the inclusion of an explicit boundary layer. The Betts-Miller scheme obtains the convective tendencies from

$$Q_c = \frac{T^c - T}{\tau_c}, \quad \langle T^c - T \rangle > 0 \quad (47)$$

$$Q_q = \frac{q^c - q}{\tau_c}, \quad \langle q^c - q \rangle > 0 \quad (48)$$

with T^c, q^c reference profiles towards which convection adjusts the temperature and moisture structure. Here, we use the linearized moisture closure option of QTCM1, i.e., we choose

$$T^c(p) = T_r^c(p) + A_1(p)(h_b + \delta h_b), \quad (49)$$

$$q^c(p) = q_r^c(p) + B_1(p)(h_b + \delta h_b), \quad (50)$$

where $h_b = s_b + q_b$, and δh_b is an adjustment which serves the dual purposes of insuring energy conservation and crudely mimicking the effects of convective downdrafts. The reference basis functions $A_1(p)$, $B_1(p)$ can in general be different from $a_1(p)$ and $b_1(p)$, though in the implementation here we will set the former equal to the latter for simplicity. With these choices, projection on the free tropospheric equations gives the free tropospheric mean heating and moistening:

$$\langle Q_c \rangle^F = \epsilon_c [\langle A_1 \rangle^F (h'_b + \delta h_b) - \langle a_1 \rangle^F T_1 + \langle T_r^c \rangle^F - \langle T_r \rangle^F], \quad (51)$$

$$\langle Q_q \rangle^F = \epsilon_c [\langle B_1 \rangle^F (h'_b + \delta h_b) - \langle b_1 \rangle^F q_1 + \langle q_r^c \rangle^F - \langle q_r \rangle^F], \quad (52)$$

with an additional switch condition below; $\epsilon_c = \tau_c^{-1}$ is a large damping rate for the dissipation of bouyancy by convection. In the boundary layer, since by construction δh_b is an adjustment to the moist static energy, we have

$$\langle Q_c \rangle^b + \langle Q_q \rangle^b = \epsilon_c [(h'_b + \delta h_b) - h'_b] = \epsilon_c \delta h_b. \quad (53)$$

At this stage, we still do not have $\langle Q_c \rangle^b$ or $\langle Q_q \rangle^b$ separately, only their sum. To obtain δh_b , we apply the energy constraint that the net moisture loss must equal the net (dry) enthalpy gain:

$$p_B (\langle Q_c \rangle^b + \langle Q_q \rangle^b) + p_F (\langle Q_c \rangle^F + \langle Q_q \rangle^F) = 0. \quad (54)$$

Combining (51), (52), (53), and (54) and solving for δh_b , we obtain

$$\delta h_b = \frac{[-(\langle A_1 \rangle^F + \langle B_1 \rangle^F) h'_b + \langle a_1 \rangle^F T_1 + \langle b_1 \rangle^F q_1 + (\langle T_r \rangle^F - \langle T_r^c \rangle^F) + (\langle q_r \rangle^F - \langle q_r^c \rangle^F)]}{(p_B/p_F) + (\langle A_1 \rangle^F + \langle B_1 \rangle^F)}. \quad (55)$$

The convective scheme is only activated when doing so would result in a positive net convective heating, $(p_F \langle Q_c \rangle^F + p_B \langle Q_c \rangle^b) > 0$, or explicitly

$$p_F [\langle A_1 \rangle^F (h'_b + \delta h_b - T_1) + \langle T_r^c \rangle^F - \langle T_r \rangle^F] + p_B \delta h_b > 0, \quad (56)$$

with δh_b given by (55).

As mentioned above, we still need to partition the net boundary layer moist static energy source to obtain $\langle Q_c \rangle^b$ and $\langle Q_q \rangle^b$. At this stage, we choose the crude device of using a fixed, constant partitioning,

$$\langle Q_c \rangle^b = \epsilon_c \delta s_b, \quad \delta s_b = \sigma \delta h_b, \quad (57)$$

$$\langle Q_q \rangle^b = \epsilon_c \delta q_b, \quad \delta q_b = (1 - \sigma) \delta h_b, \quad (58)$$

where σ is a prescribed constant. One slightly more sophisticated alternative would be to adjust the ABL towards a state of constant relative humidity, with the actual temperature and specific humidity determined by the closure. In practice this was found to lead in common circumstances to a warming of the ABL by deep convection, which is unphysical. The present formulation at least insures that deep convection always both cools and dries the boundary layer. We choose $\sigma = 0.2$, broadly consistent with observations. σ is admittedly a free parameter, but small variations (within the range 0.15-0.3) have no significant impact on the simulations.

Table 1 Model parameter values.

parameter	value	Definition
p_s, p_e, p_t	1000, 900, 200 hPa	Pressures at nominal surface, ABL top, and model top (tropopause)
\hat{a}_1, a_{1e}	0.4243, 0.2931	Vertical integral and ABL top value of temperature basis function
\hat{b}_1, b_{1e}	0.2406	Vertical integral and ABL top value of moisture basis function
\hat{a}_1^+	0.2445	
$\langle a_b^+ \rangle^b, a_b^{+e}$	0.0512, 0.1038	
$\langle V_1^2 \rangle, \langle V_1^3 \rangle / \langle V_1^2 \rangle$	$3.67 \times 10^{-2}, 0.0860$	
V_{1e}	-0.2121	
q_{re}, T_{re}	$40.59^\circ K, 294.0^\circ K$	ABL top values of reference profiles of moisture and temperature
M_{sr1}, M_{sr0}	$3.60^\circ K, 13.40^\circ K$	Reference dry static stability for baroclinic and barotropic mode
M_{sp1}, M_{sp0}	$4.040 \times 10^{-2}, 0.09$	Dry static stability change per T_1 change for baroclinic and barotropic mode
M_{qr1}, M_{qr0}	$3.00^\circ K, 23.3^\circ K$	Reference gross moisture stratification for baroclinic and barotropic mode
M_{qp1}, M_{qp0}	$3.78 \times 10^{-2}, 0.43$	Gross moisture stratification change per T_1 change for baroclinic and barotropic mode
ϵ_{1i}	7.58×10^{-2}	Frictional damping rate on baroclinic mode
ϵ_b	$1d^{-1}$	ABL drag coefficient
τ_m	$16d$	Turbulent mixing rate into free troposphere across ABL top
τ_c	$0.3d$	Convective time scale
σ	0.2	Constant partitioning between convective cooling and drying of ABL
τ_R	$30d$	Radiative time scale
Q_{Rb0}, τ_{Rb}	$-0.5^\circ K d^{-1}, 2d$	ABL background radiative heating, ABL radiative time scale
k_q, k_v	$2 \times 10^{-5} m^2 s^{-1}$	Diffusivity for moisture and meridional velocity

The expressions (55) and (56) can be simplified by choosing $T_r^c = T_r$ and $q_r^c = q_r$, but it is helpful to keep them in the more general form. The reference profiles appear in other model equations and it is important to retain consistency. We use the choices

$$\langle T_r^c \rangle^F = \langle T_r \rangle^F + q_{rb} - q_{rs} + s_{rb} - T_{rs}, \quad (59)$$

$$\langle q_r^c \rangle^F = \langle q_r \rangle^F + q_{rb} - q_{rs} + s_{rb} - T_{rs}, \quad (60)$$

where q_{rs} and T_{rs} are surface values of the original QTCM basis functions. These surface values are not otherwise used in the model. While again we can simplify the expressions by choosing $q_{rb} = q_{rs}$ and $s_{rb} = T_{rs}$, and we do in fact do so, the formulations (59) and (60) make the convection scheme otherwise independent of the choice of reference profiles, a useful property.

4 Simulation design

We use an idealized simulation design to study the dynamics of ITCZs. Idealizing the ITCZ as a narrow, zonally oriented feature, our simulations are axisymmetric, $\partial_x = 0$. The lack of zonally varying disturbances of any kind is a strong constraint which must be kept in mind as we interpret the results.

Axisymmetry does simplify the solution of the equations. It implies that the zonal (x) component of the flow, u_b, u_1, u_0 is nondivergent, while the meridional (y) component, v_b, v_1, v_0 is irrotational. This particularly simplifies the solution for the surface geopotential gradient, as described in section 2.3.

We use a fixed-SST lower boundary condition. The SST is

$$T_s = T_{s0} + \Delta T_s \exp\left[\frac{(y - y_0)^2}{\sigma_y^2}\right]. \quad (61)$$

One set of simulations includes planetary rotation, represented by an equatorial β -plane, $f = \beta y$ with $\beta = 2 \times 10^{-11} m^{-1} s^{-1}$. For these rotating simulations we choose $T_{s0} = 22^\circ C$, $\Delta T_s = 8^\circ C$, $y_0 = 800 km$, $\sigma_y = 1000 km$. This forces a hemispherically asymmetric circulation with a strong ITCZ in the northern hemisphere, and a dry southern tropics. All simulations are run to steady state, and we then examine only the steady solutions. No simulation failed to reach steady state (perhaps because of the neglect of the wind dependence of surface fluxes). The radiative equilibrium temperature $T_R = -50^\circ C$ (relative to T_r). The boundaries of the domain are rigid walls at $y = \pm Y$ with $Y = 5000 km$. For the rotating case, solutions reach a state of radiative-convective equilibrium at values of $|y|$ less than Y ,

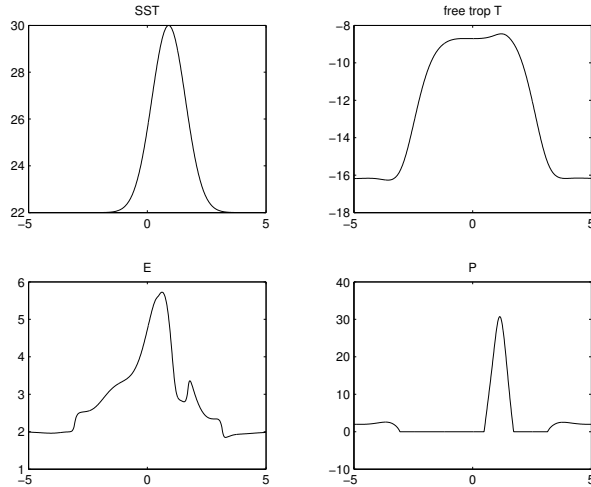


Fig. 1 Sea surface temperature ($^{\circ}C$), free tropospheric temperature ($^{\circ}C$), surface evaporation ($mm\ d^{-1}$), and surface precipitation ($mm\ d^{-1}$), for the rotating case. The horizontal axis is meridional distance, y , in thousands of km.

so there is no flow at the boundaries and the boundary conditions do not influence the flow in the interior, as was verified by sensitivity tests using larger domains.

For our nonrotating simulations, $\beta = 0$, and we use $y_0 = 0$ and $\Delta T_s = 4^{\circ}C$; other parameters are the same as the rotating case.

The equations are solved using a leapfrog differencing in time with a Robert-Asselin filter, and finite differences in space. The free tropospheric equations are solved in advective form using first-order upwind differencing, the ABL equations in flux form with a centered scheme. The horizontal grid has 800 grid points for a grid spacing of 12.5 km, much smaller than the spatial scale of the SST boundary condition and small enough so that numerical diffusion due to the first-order upwind scheme is irrelevant to the solutions, as has been checked by sensitivity experiments.

5 Results

5.1 Rotating case

Fig. 1 shows the sea surface temperature T_s , free tropospheric temperature T_1 , surface evaporation E , and surface precipitation P , as functions of latitude. The precipitation has a strong peak, the ITCZ, a large region of zero precipitation in the “winter” hemisphere ($y < 0$), and a smaller region of zero precipitation in the “summer” hemisphere ($y > 0$). Poleward of these dry regions the solutions reach radiative-convective equilibrium (RCE), with $E = P$. The free tropospheric temperature has a broad maximum, with weak variations within the region in which the solution departs from RCE and strong gradients on the boundaries of this region. All this is typical of axisymmetric Hadley cell solutions, and is qualitatively similar to such solutions of the original QTCM (Burns et al., this volume) but with a stronger ITCZ.

Fig. 2 shows the free tropospheric humidity, q_1 , baroclinic meridional velocity v_1 , baroclinic zonal velocity u_1 , and total zonal velocity at the model top, p_t , computed as $u_0 + V_1(p_t)u_1$. This last quantity shows, near the equator, the approximately parabolic structure corresponding to near-conservation of angular momentum in the Hadley circulation at this level, for reasons explained by Burns et al. (2005, this volume). In interpreting v_1 and u_1 , remember that the basis function is negative in the lower troposphere, so the plot has the sign of the actual physical velocity in the upper troposphere. The free tropospheric humidity shows a sharp peak at the location of the precipitation maximum in the previous figure, and a drier region, below the RCE value, in the winter hemisphere. q_1 is not suppressed below the RCE value in the precipitation-free region in the summer hemisphere.

Fig. 3 shows the ABL specific humidity, q_b , dry static energy, s_b , meridional velocity, v_b , and zonal velocity, u_b . Notice that the maximum in s_b is much sharper than that in T_1 . This is a consequence

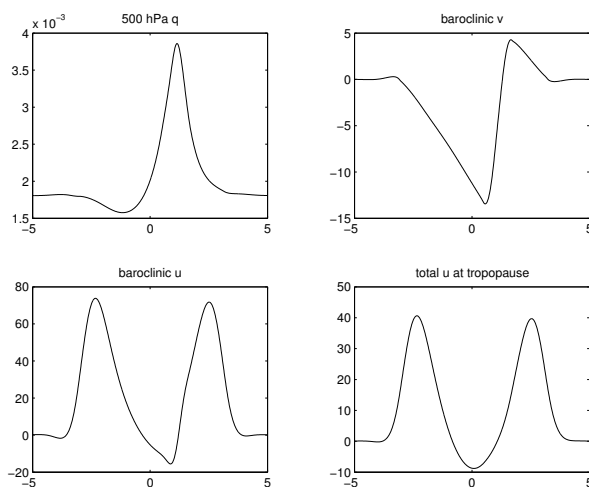


Fig. 2 Free tropospheric humidity, baroclinic meridional velocity v_1 , baroclinic zonal velocity, and total zonal velocity at the nominal tropopause pressure, p_t , for the rotating case. Note that v_1 is signed in the direction of the upper tropospheric flow.

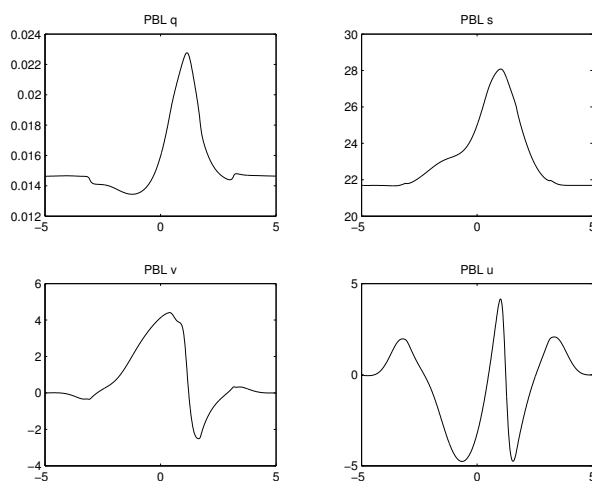


Fig. 3 Boundary layer moisture, dry static energy, meridional velocity, and zonal velocity, for the rotating case.

of the much larger drag on the ABL flow than on the free tropospheric flow; the weak temperature gradient approximation can be useful for the free tropospheric circulation, but not the ABL circulation (Sobel and Bretherton 2000; Shaevitz and Sobel 2004). The ABL zonal velocity shows a strong (for the surface) westerly jet on the equatorward flank of the ITCZ, weaker easterly jets on either side of it, and still weaker westerlies at the poleward boundaries of the Hadley circulation. The westerly jet is sharp enough to locally reverse the absolute vorticity gradient, so that the ITCZ would be barotropically unstable to zonally varying disturbances (if those were allowed in the model), as may at times be the case for the real eastern Pacific ITCZ (Nieto Ferreira and Schubert 1997; Wang and Magnusdottir 2005).

5.2 Nonrotating case

Fig. 4 shows the nonrotating simulation. In the absence of any Coriolis force, a given meridional pressure gradient results in a larger meridional velocity than it would in the rotating case, and consequently the same SST gradient results in a larger precipitation maximum in the nonrotating than the rotating case. The reduction in our imposed SST gradient by a factor of two compared to the simulations

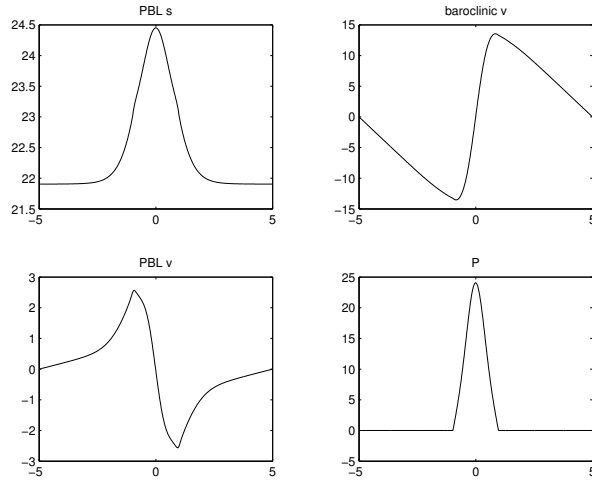


Fig. 4 Boundary layer dry static energy, free tropospheric meridional velocity, boundary layer meridional velocity, and precipitation, for the nonrotating case.

above, $\Delta T_s = 4^\circ C$, roughly compensates for this. Without rotation, the circulation is better described as a Walker type or “mock Walker” circulation (Grabowski et al. 2000; Bretherton and Sobel 2002; Bretherton et al., this issue). Since the deformation radius is infinite without rotation, the circulation fills the domain, and thus is not independent of domain size. The equator has no particular dynamical meaning in this non-rotating case, so placing our SST maximum off the equator would only mean that the flow would be asymmetric with respect to the boundaries. Our placement of the forcing at $y = 0$ in this case is just the simplest choice.

For brevity, we do not show all the fields shown for the rotational case in section 5.1 (note also that steady solutions to the nonrotating case have no zonal winds, since there are no zonal pressure gradients due to axisymmetry). Fig. 4 shows ABL dry static energy s_b , free tropospheric baroclinic meridional velocity v_1 , boundary layer meridional velocity v_b , and precipitation P . Both meridional velocities now decrease in absolute magnitude from peaks on the flanks of the SST maximum to the boundaries. They decrease differently, though, with v_1 being nearly linear, much as in Walker solutions under the weak temperature gradient approximation (Bretherton and Sobel 2002; Sobel et al. 2004) and v_b being more trapped near the SST maximum.

5.3 Boundary layer meridional momentum budgets and the validity of the Lindzen-Nigam model

Given the debate regarding the different mechanisms for forcing flow in the boundary layer (e.g., Wu et al. 1999, 2000; Chiang et al. 2001; Bacmeister and Suarez 2002), it is of interest to examine the meridional momentum budget there. The meridional component is of most interest here since it is that one which couples strongly to the thermodynamic budgets and thus the precipitation field. Figs. 5 and 6 show these budgets for the rotating and nonrotating case respectively.

We wish to isolate the contribution to the pressure gradient which is determined hydrostatically by the ABL temperature gradient, since that drives the flow in the LN model. The total pressure gradient term appearing in the v_b equation is $-\partial_y(\kappa\langle a_b^+ \rangle^b s_b + \phi_s)$, but ϕ_s has a contribution from s_b as well. Rewriting (31) schematically, with the gradient of ϕ_s alone on the left-hand side,

$$\partial_y \phi_s = -\partial_y(\kappa a_b^{+e} s_b + \kappa \langle a_1^+ \rangle^F T_1) + \dots \quad (62)$$

where the ellipsis represents other terms. Thus the total sum of all pressure gradient terms on the RHS of the meridional component of (25) can be written

$$-\partial_y[\kappa(\langle a_b^+ \rangle^b - a_b^{+e})s_b - \kappa T_1 + \dots].$$

The term in s_b is what we call the LN contribution, while the rest, including the term in T_1 as well as other, essentially barotropic contributions to ϕ_s , is the free tropospheric contribution to the ABL

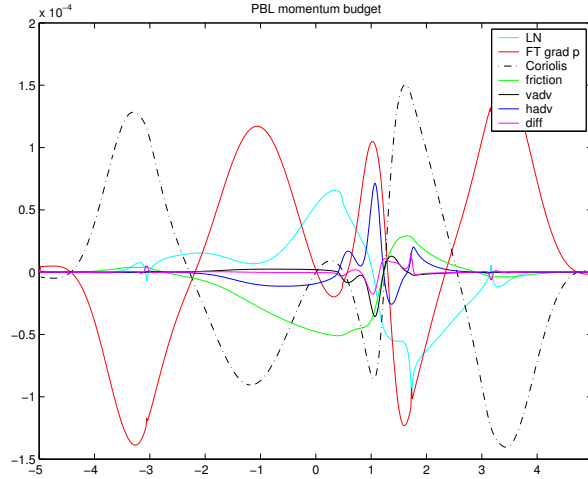


Fig. 5 Boundary layer meridional momentum budget for the rotating case, showing LN (see text) and free tropospheric contributions to the pressure gradients, as well as the Coriolis, friction, vertical and horizontal advection (marked vadv and hadv, respectively), and diffusion terms.

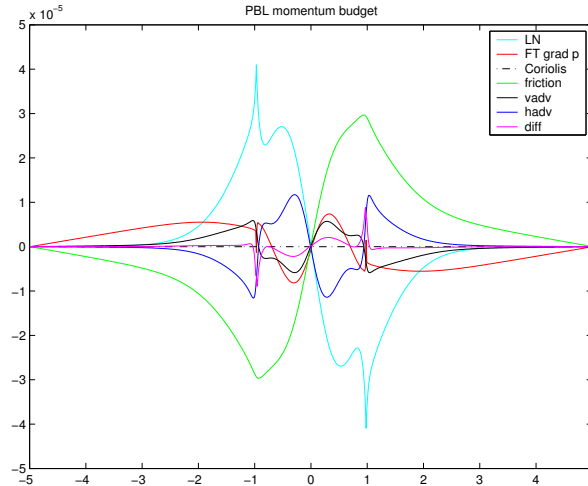


Fig. 6 Boundary layer meridional momentum budget for the nonrotating case, showing LN (see text) and free tropospheric contributions to the pressure gradients, as well as the Coriolis (zero in this case), friction, vertical and horizontal advection, and diffusion terms.

pressure gradient. These two contributions are plotted separately in figs. 5 and 6, along with the Coriolis, friction, vertical and horizontal advection, and diffusion terms.

In the nonrotating case (Fig. 6), the dominant balance is between the LN term and friction. Since the friction term depends (linearly in our model) on v_b itself, it is fair to say that v_b is largely determined by LN dynamics. We note that the $\partial_y s_b$ term looks significantly different than $\partial_y T_s$, so this is not the LN model per se but a generalization consistent with its overall intent. In the rotating case, the situation is more subtle. Particularly away from the equator, the dominant balance is geostrophic, between the free-tropospheric pressure gradient and Coriolis term, with the LN term being relatively small. At and near the spot to the south of the ITCZ where v_b actually attains its maximum value, however, the LN-friction balance is still locally an important contributor. Over a larger region around the ITCZ on both sides, while the free tropospheric pressure gradient and Coriolis terms become large, they have a large degree of cancellation between them and the LN and friction terms broadly resemble each other in structure and magnitude, suggesting a causal relation. Horizontal advection becomes important in a narrow region within the ITCZ, as might be expected since the gradient of v_b is largest there.

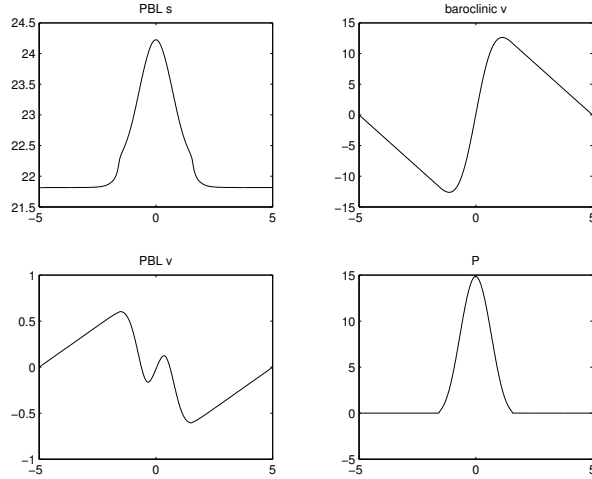


Fig. 7 Boundary layer dry static energy, free tropospheric meridional velocity, boundary layer meridional velocity, and precipitation for an irrotational case with the LN terms removed from the boundary layer meridional momentum budget (see text for details). Compare to Fig. 4.

Besides budget diagnostics, another way to examine the importance of a physical process to a model solution is to remove that process from the model and examine the solution to the modified model. Fig. 7 shows, in the same format as Fig. 4, a solution to a nonrotating case in which the LN terms have been removed from the ABL momentum budget. Comparing this solution to the control case shown in Fig. 4, v_b is dramatically reduced, as we would expect based on the diagnostics shown in Fig. 6. Its structure is also altered, with a narrow region of ABL divergence now appearing in the center of the ITCZ. At the same time, the free-tropospheric meridional velocity, v is almost unaltered. The precipitation is reduced by a bit less than 40%. This reduction leads us to conclude that for this case, the LN terms contribute significantly to the ITCZ precipitation, but are not quite the dominant player in determining it. Presumably, weak temperature gradient arguments of the sort given by Bretherton and Sobel (2002) and Sobel et al. (2004), for a case very similar to this in the standard QTCM (with no ABL), and elaborated on more broadly by Sobel and Bretherton (2000) and Shaevitz and Sobel (2004), can be used to understand the solution which remains in the absence of the LN terms.

In the rotating case, not shown here, the effect of removing the LN terms is similar to, but a bit smaller than that for the nonrotating case of Fig. 7. The structure of v_b is changed similarly, with a narrow region of divergence introduced in the core of the ITCZ, but the overall magnitude of v_b is reduced by less than it is in the nonrotating case, and the precipitation is reduced by around 25%.

5.4 Sensitivity to horizontal moisture diffusivity

The rotating simulation shown in Fig. 1 has a peak precipitation in the ITCZ much larger than any observed in earth’s climatology, despite an SST contrast whose magnitude is arguably comparable to those found on earth (arguable because it is not obvious precisely how to compare our idealized SST structure with the real structure of earth’s SST field). However, this peak precipitation is a strong function of the horizontal diffusivity of moisture. This is shown in Fig. 8, which compares the control simulation’s precipitation field to those from simulations in which this diffusivity is doubled and halved. A lower diffusivity leads to a stronger, narrower ITCZ. The total integrated precipitation over the ITCZ is very similar in all three simulations shown; because the lower boundary condition is fixed SST, the surface evaporation (and thus the domain-integrated precipitation) can and does vary slightly between simulations, and this is responsible for a small part of the difference.

From this picture one might guess that the nondiffusive limit of these equations could be singular, with continued narrowing and intensification of the ITCZ as the diffusivity goes to zero. The results in section 6 show that this is not the case under a particular set of simplifying assumptions. Nonetheless, the behavior of the present model appears quite different from that of the original QTCM equations,

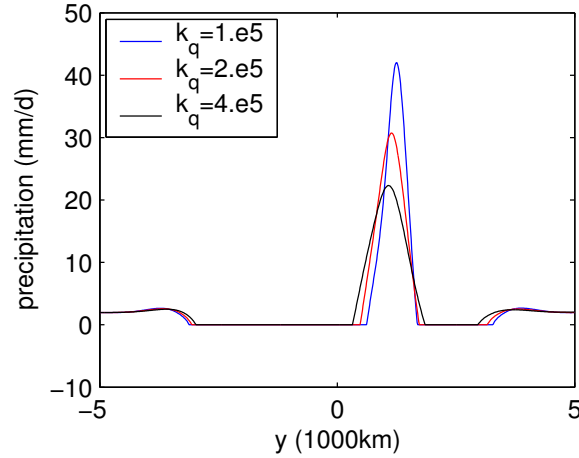


Fig. 8 Precipitation for rotating solutions with horizontal moisture diffusivity equal to 1, 2, and $4 \times 10^5 \text{ m}^2 \text{ s}^{-1}$ (where 2×10^5 is the standard in other runs).

which produce an ITCZ of quite moderate width and intensity in the absence of any diffusion whatsoever (Burns et al. 2005, this volume). In the present model, although the same diffusivity is applied to free-tropospheric and ABL humidity as well as ABL dry static energy, sensitivity tests (not shown) demonstrate that it is the diffusion of free-tropospheric humidity which controls the ITCZ intensity and width. Moist static energy budget analysis in section 7 suggest that this has much to do with the model solution's occurring in a regime in which (as is usually assumed) the tropospheric gross moist stability is small compared with the dry static stability.

6 Analytical case

In this section we present analytical results under a number of simplifying assumptions that highlight the role of the boundary layer and provide insight into the causes of the strong convergence zone seen in the numerical results of section 5. We first take the convective quasi-equilibrium (QE) limit, in which τ_c is small compared to other time scales. We then use assumptions of weak barotropic pressure gradient and weak temperature gradient (WTG) in the free troposphere. If we then for exposition purposes neglect some moisture and dry static energy transport terms (which are important in the numerical simulations), we find a solution that has many parallels to the simple model of Lindzen and Nigam (1987), and which yields a large but finite convergence driven from the ABL. For simplicity, we use the nonrotating case, with $u = 0$, retaining y as the spatial coordinate, though as noted above, this analysis applies equally well to a mock-Walker circulation in which longitude is the coordinate. Under these conditions, we can obtain the most relevant elements of the solution by considering only the convecting region, assumed to have finite width.

6.1 ABL dynamics and thermodynamics

Within convecting regions, for upstream vertical advection, and assuming τ_m terms are switched off (or negligible) in the thermodynamic equations, with the surface flux, radiative, and convective parameterizations (43), (45), (46), through (57) and (58), the ABL dry static energy and moisture equations (23) and (24) become

$$(\partial_t + v_b \partial_y - k_q \partial_y^2) s_b = \tau_s^{-1} (T_s - s_b) + Q_{Rb0} + \tau_{Rb}^{-1} (T_s - s_{rb} - s_b) + \epsilon_c \sigma \delta h_b \quad (63)$$

and

$$(\partial_t + v_b \partial_y - k_q \partial_y^2) q_b = \tau_s^{-1} (q^*(T_s) - q_b) + \epsilon_c (1 - \sigma) \delta h_b, \quad (64)$$

where τ_s is defined by (44). It proves useful to eliminate $\epsilon_c \delta h_b$ terms between (63) and (64). This yields

$$(\partial_t + v_b \partial_y - k_q \partial_y^2)[(1-\sigma)s_b - \sigma q_b] = \tau_s^{-1}[(1-\sigma)(T_s - s_b) - \sigma(q^*(T_s) - q_b)] + (1-\sigma)(Q_{Rb0} + \tau_{Rb}^{-1}(T_s - s_{rb} - s_b)) \quad (65)$$

This manipulation is motivated by the convective QE limit examined below, but does not itself involve approximations. Its effect is similar to the use of the moist static energy equation when considering the whole troposphere, in that it eliminates the convective terms in the individual equations. While the moist static energy equation holds independent of the specific convective parameterization because it is derived by integrating over the entire depth of convection, the ABL equation (65) depends on the parameterization, specifically on the partitioning of moistening and cooling in the ABL, controlled by σ . The quantity $[(1-\sigma)s_b - \sigma q_b]$ is unaffected by the convective terms in the present parameterization.

Turning to the convective QE limit of small τ_c , with $\epsilon_c = \tau_c^{-1}$, (57) and (58) imply $\delta h_b \leq O(\tau_c)$. Using this in (57) and (58), taking the sum of nonconvective terms in (32) and (33) to be $O(1)$, yields $h'_b - T_1 = O(\tau_c)$, $h'_b - q_1 = O(\tau_c)$ where we have explicitly set $A_1 = a_1$, $B_1 = b_1$, $T_r^c = T_r$, and $q_r^c = q_r$ for simplicity as well as consistency with our numerical simulations. This also satisfies (55). The QE linkage of T_1 to h_b implies at leading order in τ_c

$$s_b + q_b = T_1 \quad (66)$$

This permits the elimination of one ABL thermodynamic variable, implying that (65) is a sufficient equation to determine ABL thermodynamics in convective QE. It also implies that (63) and (64) cannot be separately satisfied without the ABL cooling/moistening terms as $O(1)$, i.e., $\delta h_b = O(\tau_c)$ as expected.

The terms on the rhs of (65) draw s_b toward an equilibrium that tends to follow SST, while the terms on the lhs transport or smooth this. For the simplest case, we neglect the lhs and examine the consequences of the local balance. Defining

$$\tau_b^{-1} = \tau_s^{-1} + (1-\sigma)\tau_{Rb}^{-1}, \quad (67)$$

(65) then becomes

$$s_b = \tau_b \tau_s^{-1} [(1-\sigma)T_s - \sigma(q^*(T_s) - T_1)] + \tau_b (1-\sigma)(Q_{Rb0} + \tau_{Rb}^{-1}(T_s - s_{rb})) \quad (68)$$

Note that T_1 is required, although that term is small if the ABL convective cooling fraction σ is small. In the WTG limit considered below, T_1 is approximately spatially constant T_1 , set by domain average energy balance, would be required to obtain s_b , but vanishes in the gradient. in (69). For use in gradients, define $\partial_y q^*(T_s) = \gamma \partial_y T_s$.

Turning to the momentum equations, neglecting ABL momentum advection relative to surface drag, the steady ABL velocity equation (25) becomes

$$\epsilon_b \mathbf{v}_b = -\nabla(\kappa \langle a_b^+ \rangle^b s_b + \phi_s). \quad (69)$$

6.2 Free troposphere in a linear, non-rotating, WTG limit

In the \mathbf{v}_0 equation (21), the geopotential gradient term contains the sum of surface geopotential and the vertical average of baroclinic contributions from both layers. For maximum simplicity, we assume that for small enough SST forcing, the momentum advection terms can be considered small. The drag at the top of the ABL contributes terms of order τ_m^{-1} , likewise considered small. Because we obtain the relevant parts of the solution at leading order, the precise scaling of τ_m relative to τ_c is not crucial. At leading order in τ_m^{-1} , this leaves

$$\partial_y(\kappa a_b^{+e} s_b + \kappa \langle a_1^+ \rangle^F T_1 + \phi_s) = 0. \quad (70)$$

Similar neglect of the momentum advection and drag terms in the \mathbf{v}_1 equation (22) yields the WTG approximation at leading order

$$\partial_y(T_1) = 0. \quad (71)$$

In a rotating case, Ekman pumping ABL terms would add a feedback onto the tropospheric solution. We also note that some of the $O(\tau_m)$ terms if retained would be multiplied by M_B/M_1 which is greater than unity. Thus this limit is more suited to simplicity than reproduction of the numerical results.

These approximations assume that flow extends over larger space scales in the free troposphere than in the boundary layer such that the free tropospheric contribution to boundary layer pressure gradients is negligible. This is not well justified in realistic regimes, but highlights the role of the boundary layer and permits connection to the Lindzen-Nigam model. With (70) and (71), giving the ϕ_s contribution to the boundary layer equation, (69) becomes

$$\epsilon_b v_b = \kappa(a_b^{+e} - \langle a_b^+ \rangle^b) \partial_y s_b \quad (72)$$

6.3 LN contribution

The simplified ABL equations under QE (68) and (69), with the WTG conditions (70) and (71) are now solvable, yielding

$$v_b = \epsilon_b^{-1} \kappa(a_b^{+e} - \langle a_b^+ \rangle^b) [\tau_b \tau_s^{-1} ((1 - \sigma) - \sigma \gamma) + \tau_b \tau_{Rb}^{-1} (1 - \sigma)] \partial_y T_s \quad (73)$$

The divergence $\partial_y v_b$ is then proportional to $\partial_y^2 T_s$. Evaluating this using $\partial_y^2 T_s \approx 2\sigma_y^{-2} c_p \Delta T_s$, with $\sigma_y = 10^6$ m, $\Delta T_s = 8K$, τ_b/τ_s , $\tau_b/\tau_{Rb} = O(1)$, σ small, and $\kappa(a_b^{+e} - \langle a_b^+ \rangle^b) = 0.015$, yields values of divergence on the order of 10^{-5} s^{-1} . This is on the same order as climate estimates for surface convergence (Liu and Xie 2002), although the latter does not necessarily hold through as deep a layer. This SST-driven ABL convergence tends to drive a convergence contribution in the free troposphere as discussed below. Adding this to the convergence by the NZ part of the dynamics leads to large model convergence and precipitation, but the solution is clearly nonsingular. The ABL convergence driven by pressure gradients due to ABL temperature following SST is very much akin to the LN solution, justifying referring to this as the LN contribution.

Considering the terms on the lhs of (63), assuming the same y -scale, suggests the $v \partial_y s_b$ term is of the same order as the terms on the rhs. The numerical solutions indicate that these terms (not shown) do modify the s_b pattern noticeably compared to that of the SST (e.g., Fig. 3b, Fig. 4a). Thus even in what we are calling the LN contribution, thermodynamics does matter. Diffusion becomes important only where the y -gradients become substantially larger than that of the underlying SST. The numerical solutions also indicate that the neglect in (70) and (71) of ABL pressure gradients due to the free tropospheric temperature and the barotropic mode are not well justified under realistic model parameters. Rather they should be interpreted as a means of obtaining the LN case (73), which is useful both for its historical value and conceptual simplicity.

The ABL equation with convective heating eliminated (65) or the analytical case (73) point to potential sensitivity of boundary layer solutions to how boundary layer cooling and moistening is treated in GCM convective parameterizations. If the portion of ABL moist static energy adjustment that goes into cooling the ABL is a small fraction of the portion that goes into moistening it (i.e., small σ in the simple parameterization used here), then this sensitivity is small. For cooling fraction approaching 1, the steady precipitating ITCZ in QE and WTG approximations used in (73) would yield cold s_b over warm SST, provided that NZ contributions maintained precipitation. While cooling of the ABL by convection is a well-known process contributing to finite lifetimes of some convective events, a parameterization with a large cooling fraction would either have to spend a smaller fraction of the time convecting or have ABL solutions that departed from following SST in convective regions.

7 Interpretation

Here we turn back to the numerical results, interpreting them in light of the analytical results obtained above. Consider (39), with tendency and horizontal advection terms written schematically as “adv” and “diff”. Focussing on vertical advection terms is justified near the maxima of precipitation and moisture in center of the ITCZ, since horizontal gradients are small there. Because the terms in $\nabla \cdot \mathbf{v}_b$ are strongly determined by ABL balances, we move them to the right-hand side, to obtain

$$p_F M_1 \nabla \cdot \mathbf{v}_1 + \text{adv} + \text{diff} = p_B M_B \nabla \cdot \mathbf{v}_b + g F_{net}, \quad (74)$$

where F_{net} is the net input of moist static energy to the whole troposphere due to surface fluxes and radiation, and M_B is given by (40). This equation is similar to that which would be obtained from a moist static energy budget analysis of the QTCM, or for that matter two-layer models such as that of

Neelin and Held (1987), which would have a baroclinic divergence times a gross moist stability equal to the sum of surface fluxes and vertically integrated radiative cooling. In such an analysis, the surface fluxes and radiation are regarded as driving the divergent flow, against an effective stratification for the total moist flow given by the gross moist stability. Variations in precipitation from the radiative-convective equilibrium value are approximately proportional to the divergent flow thus forced. The difference here is the first term on the right-hand side. This is the import of moist static energy due to the divergent component of the ABL/barotropic mode. It is import, rather than export, in regions of ABL mass convergence if M_B is negative in such regions. This tends to be the case because generally $h_e < h_b$, and M_0 is negative for typical q_1 .

Although diagnostic, (74) is written in a form suggestive of a causal interpretation. To the extent that $\nabla \cdot \mathbf{v}_b$ is determined by the ABL dynamics of section 6, it can be viewed as a forcing, similarly to the net flux term. Strictly speaking, the latter is coupled to the flow as well, but because it tends to react on larger spatial scales, it can be approximated as externally imposed. Thus, we can understand the role of boundary layer momentum dynamics as driving \mathbf{v}_b divergence, providing the moist static energy import term $M_B \nabla \cdot \mathbf{v}_b$ which, in turn, forces a contribution to the baroclinic divergence as described above. The $\nabla \cdot \mathbf{v}_1$ contribution is important because it yields much of the moisture convergence that produces precipitation. Thus there exists a set of conditions under which the first term on the rhs of (74) yields the LN contribution, while the second yields the NZ contribution. Although in general there will be a part of $\nabla \cdot \mathbf{v}_b$ that acts as a feedback on the free tropospheric solution, the analytical results presented above make explicit the assumptions necessary to obtain a neat separation, by showing how to arrive at a solution in which v_b is entirely determined by T_s .

Fig. 9a shows the breakdown of (74), in which the horizontal advection terms are included with the associated M_1 and M_B terms. The curve labeled ‘‘ABLx flux divergence’’ is the total vertically integrated flux divergence due to v_b , v_0 , and the vertical motion associated with their divergence, while the curve labeled ‘‘BC flux divergence’’ is the flux divergence due to the baroclinic meridional flow, v_1 . Surface fluxes, radiation, and horizontal diffusion are the other terms in the budget. All terms are computed as vertical (pressure) mean tendencies, with the ABL and free-tropospheric contributions weighted appropriately. We see that the dominant balance in the ITCZ is between horizontal diffusion and barotropic flux divergence, with surface fluxes and radiation being dominant away from the ITCZ, and significant but smaller than diffusion and barotropic divergence in the ITCZ. Baroclinic flux divergence, associated with the baroclinic gross moist stability M_1 , is everywhere relatively small. This small M_1 -regime is associated in part with the high moisture in the ITCZ region (Fig. 2a), since the gross moist stability is determined by the flow in a non-trivial manner. The horizontal advection terms, not shown separately, contribute significantly to the flux divergences only on the flanks of the ITCZ, being essentially negligible elsewhere.

To test how the budget changes with parameters that affect M_1 , Fig. 9b shows the same figure for a case where M_{sr1} has been increased by $c_p \times 0.7$ C. In this case, the baroclinic flux divergence is a significant negative (moist static energy export) contribution in a relatively broad region through the ITCZ. Moisture diffusion still has a larger peak value. ITCZ precipitation has decreased by about 10-15% in this run, relative to the standard.

To the extent that this model has validity, the result that strong horizontal diffusion is needed to obtain realistic ITCZ precipitation is provocative. There is of course no horizontal diffusion of the magnitude we use in the real atmosphere. Given our axisymmetric formulation, it may be reasonable to interpret the diffusion as representing transport by longitudinally varying disturbances. It seems likely that the most important such disturbances in the ITCZs are transients, such as easterly waves, although since all real ITCZs are finite in zonal extent, it is also possible that time-mean zonal advection could play a part in ventilating the ITCZ with lower moist static energy air from adjacent regions. To the extent that transients dominate, however, the implication of our results is that such disturbances play an essential role in the time-averaged thermodynamics of the ITCZ. Transients have been invoked as important to the ITCZ before, but not by this mechanism. This is consistent with results of a full QTCM that has two vertical basis functions in moisture, while the rest of the discretization remains as in NZ (Neggers et al 2005). Free tropospheric moisture, being less tied to SST, has much more variability and larger impact of moisture transients (for realistic shallow convective time scales) than when a single q basis function is used. For the same reasons, free tropospheric moisture is much higher in ITCZs than in descent regions, decreasing M_1 and increasing ITCZ intensity.

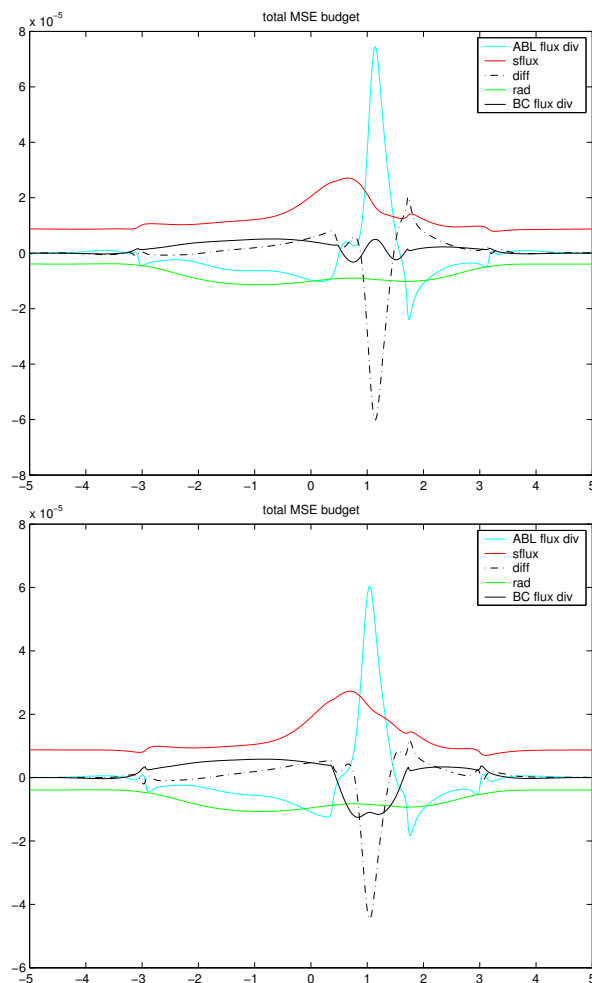


Fig. 9 Vertically integrated moist static energy budget for the rotating case. Terms plotted are the total flux divergence associated with M_0 due to the ABL (plus related barotropic component of the free tropospheric flow), denoted ABL flux div; flux divergence associated with M_1 due to the baroclinic component of the free tropospheric flow, denoted BC flux div; surface fluxes (*sflux*); radiation (*rad*); and horizontal diffusion (*diff*). All terms expressed as tendencies, in s^{-1} . (a) Standard case. (b) Sensitivity experiment in which M_1 is increased by increasing M_{sr1} .

One may ask whether the moist static energy convergence due to the ABL mode is artificially large due to the choice of vertical structures. In the absence of deep convection, ABL convergence should probably be vented in a shallow return flow just above the ABL (Zhang et al. 2004; McGauley et al. 2004) rather than in a deep return flow. However, a lower return flow will be nearer the lower tropospheric moist static energy minimum which occurs in most tropical soundings, and this will only make the gross moist stability associated with this flow *more negative* than our M_0 [see, e.g., Neelin (1997) for a heuristic discussion of the relationship between the gross moist stability and the vertical profiles of vertical velocity and moist static energy], increasing the import of moist static energy by ABL convergence. One might speculate that inclusion of a second baroclinic mode, associated with heating by stratiform anvil clouds of large mesoscale convective systems, could modify the picture because convergence at midlevels where moist static energy is low would imply a strongly positive gross moist stability. However, the ITCZ in reanalysis data has a relatively low maximum in vertical velocity (M. Biasutti, personal comm. 2005), so the picture here appears very plausible.

8 Conclusions

We have formulated a model for the study of the narrow ITCZs, idealized as steady, axisymmetric structures. Our model has a truncated vertical structure consisting of a free troposphere with two modes, based on the baroclinic and barotropic modes of the QTCM, and a slab mixed layer underneath it. We have focused particularly on the interaction of the momentum dynamics of the ABL and the thermodynamics of the free troposphere in determining the width of the ITCZ and the maximum precipitation rate occurring at its core.

Within this model framework, one can identify a role for baroclinic pressure gradients associated with ABL temperature tending to follow SST, the mechanism postulated by LN. While there is a larger role for thermodynamics in determining these pressure gradients than in the original LN model, it is appropriate to refer to their effect on the flow and precipitation as the LN contribution. The contribution arising from the dynamics present in the NZ QTCM is referred to as the NZ contribution. Under certain approximations, the LN contribution can be examined analytically. In model budget analysis of ABL momentum equations, the contribution to pressure gradients by LN terms can be substantial, particularly in the nonrotating case. In the rotating case, the LN terms are important at smaller scales close to the ITCZs. In neither case do these terms actually determine the precipitation to the extent that the ABL momentum budgets might suggest. Evaluation of the overall impact of the LN terms on the flow, including on precipitation, was conducted by suppressing these terms in numerical experiments. The overall impact of this suppression on the precipitation is a reduction on the order of 25-40%, depending on the particular case. While the NZ contribution is larger, this suggests that the LN contribution can be quantitatively important to sharp ITCZs.

The model tends to produce very strong ITCZs in this zonally symmetric case, with rainfall that is larger than observed. The large rainfall values may be to some extent associated with the zonal symmetry, since zonally symmetric versions of the NZ QTCM give values comparable to observed (Burns et al., this volume), while the three dimensional (3-D) version has weak ITCZs. A clear difference is large transient eddy fluxes of moisture to midlatitudes in the 3-D case, increasing midlatitude precipitation at the expense of tropical.

Although the LN contribution appears not to make the equations singular, the sharp ITCZ in the zonally symmetric case tends to result in diffusion terms being important to limiting peak precipitation values. The role of diffusion is interpreted as pointing to the likely role of transients in the 3-D case. The importance of diffusion in the MSE budget is to a modest extent associated with the very small, or in some cases even slightly negative, values of the tropospheric gross moist stability in these simulations. This in turn appears to be associated with the greater freedom in tropospheric moisture due to the introduction of the ABL. The lower tropospheric moisture tends to increase in strongly convecting regions, decreasing moist stability and increasing moisture gradients. This same effect operates in a QTCM version with the ABL-troposphere separation included only in the moisture equation, where it produces both sharper ITCZs and stronger transient moisture advection (Neggers et al 2005). The dominant effect here, however, seems to be associated with the introduction of a distinct ABL circulation.

The role of this ABL circulation may be seen in the moist static energy budget, where ABL convergence appears as an additional “forcing”, beside the net heat flux into the column. It must be balanced by some combination of the transport terms in the free troposphere, including moist static energy export associated with positive free tropospheric gross moist stability, moisture and temperature advection and diffusion terms. This provides a simple means of viewing the roles of the LN and NZ contributions. The balance between net flux and tropospheric MSE transport terms is key to the NZ contribution. Under certain approximations, the ABL term is essentially the LN ABL convergence contribution, determined by ABL balances. Because this term tends to import moist static energy, other MSE transports must compensate for it as well as balance the flux forcing, yielding LN and NZ contributions respectively. Both contributions yield baroclinic moisture convergence and precipitation. The total vertical integral of moist static energy divergence by both components together would be negative, even when the baroclinic gross moist stability is positive, consistent with recent estimates for the Pacific ITCZ (L. Back and C. Bretherton, personal communication). By separating the the negative gross moist stability contribution associated with ABL convergence and interpreting it as an additional forcing contribution, the distinct dynamical roles of the two components are clarified, and the notion of a positive gross moist stability for deep, “first baroclinic mode” flows can be made

consistent with the possibility that the total quasi-steady circulation may import moist static energy into the ITCZ.

Appendix: Sensitivity to schemes for mixing and vertical advection across ABL top

A.1. Adjustment to reference temperature above ABL top.

When the reference profiles and basis functions for the free troposphere are taken directly from the original QTCM, simply truncated at ABL top, simulations tend to develop a surface temperature slightly greater than the SST and negative sensible heat flux in some regions. While this does not cause any other significant problems in the solutions, it is undesirable. It is associated with strong entrainment of warm air from above due to the τ_m term in (23) where the model develops strong inversions. While the long term solution would be to improve ABL radiative (regions with strong inversion tend to have strong ABL cloud-top cooling) and mixing parameterizations, here we have simply compensated by reducing the value of the reference temperature profile (by about 2.5 C, horizontally constant) just above ABL top. This reduces the dry static energy, s_e , which is used for vertical advection as well as the τ_m terms in the equations for T_1 and s_b . Other, integral properties of the reference profile (e.g., $\langle T_r \rangle^F$) are not altered, assuming that only a shallow layer is modified. This removes regions of negative sensible heat flux. The sensible heat flux is in any case small compared to the latent heat flux, and the meridional profile of s_b stays similar to that of the SST whether we make this change or not. No other major features of the solutions are sensitive to this change.

A.2 Sensitivity to mixing and vertical advection switches.

Fig. 10 shows the precipitation for three solutions. One is the same shown in Fig. 1, using our control parameters. Another uses the centered scheme rather than the upwind one for advection across ABL top (see section 2.3). In the third, the mixing terms in τ_m^{-1} are shut off whenever deep convection is active. We see that all these changes have miniscule effects on the precipitation field in the tropics. This is not the only valid measure, but it is the one we are most interested in here. The boundary layer humidity (not shown) shows somewhat greater sensitivity to the vertical advection scheme. In the nonrotating case, weak stationary oscillations in the precipitation and other fields can develop in regions of weak mean descent when the mixing is turned off in the presence of deep convection; these appear to be undesirable artifacts of the on/off switches in these parameterizations. In the full implementation of the QTCM2 model formulated here, we anticipate more complete physical parameterizations, such as the shallow convection parameterization of Neggers et al (2005b, this issue).

Acknowledgements This work was supported in part by National Science Foundation grants DMS-0139666 and DMS-0139830. We thank L. Back, M. Biasutti, C. Bretherton, J. Chiang, E. Maloney, M. Peters, and the members of the Focused Research Group on tropical dynamics for discussions.

References

1. Bacmeister, J. T., and M. J. Suarez: Wind stress simulations and the equatorial momentum budget in an AGCM. *J. Atmos. Sci.*, **59**, 3051-3073 (2002).
2. Battisti, D. S., E. S. Sarachik, and A. C. Hirst: A consistent model for the large scale steady surface atmospheric circulation in the tropics. *J. Climate*, **12**, 2956-2964 (1999).
3. Betts, A. K.: A new convective adjustment scheme. Part I: Observational and theoretical basis. *Quart. J. Royal Meteor. Soc.*, **112**, 677-691 (1986).
4. Betts, A. K., and M. J. Miller: A new convective adjustment scheme. Part II: Single column tests using Gate wave, BOMEX, ATEX and arctic air-mass data sets. *Quart. J. Royal Meteor. Soc.*, **112**, 693-709 (1986).
5. Bretherton, C. S., and A. H. Sobel: A simple model of a convectively coupled Walker circulation using the weak temperature gradient approximation. *J. Climate*, **15**, 2907-2920 (2002).
6. Bretherton, C. S., M. E. Peters, and L. E. Back: Relationships between water vapor path and precipitation over the tropical oceans. *J. Climate*, **17**, 1517-1528 (2004).
7. Burns, S. P., A. H. Sobel, and L. M. Polvani: Asymptotic solutions to the moist axisymmetric Hadley circulation. *Theor. Comp. Fluid Dyn.*, submitted.

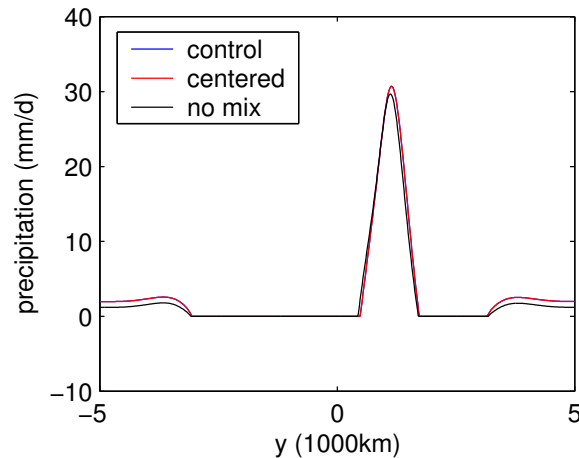


Fig. 10 Precipitation for rotating solutions using control parameters as well as a solution with the vertical advection across ABL top done using a centered rather than upwind scheme, and one in which the mixing across ABL top (the terms in τ_m^{-1}) is shut off when deep convection is active.

8. Charney, J. G., 1971: Tropical cyclogenesis and the formation of the Intertropical Convergence Zone. *Mathematical Problems in Geophysical Fluid Dynamics*, W. H. Reid, Ed., *Lectures in Applied Mathematics*, **13**, Amer. Math. Soc., 355-368.
9. Chiang, J. C. H., and S. E. Zebiak: Surface wind over tropical oceans: Diagnosis of momentum balance, and modeling the linear friction coefficient. *J. Climate*, **13**, 1733-1747 (2000).
10. Chiang, J. C. H., S. E. Zebiak, and M. A. Cane: Relative roles of elevated heating and surface temperature gradients in driving anomalous surface winds over tropical oceans. *J. Atmos. Sci.*, **58**, 1371-1394 (2001).
11. Chou, C. and J. D. Neelin: Mechanisms of global warming impacts on regional tropical precipitation. *J. Clim.*, **17**, 2688-2701 (2004).
12. Davey, M. K., and A. E. Gill: Experiments on tropical circulation with a simple moist model. *Q. J. R. Meteorol. Soc.*, **113**, 1237-1269 (1987).
13. Emanuel, K.A.: An air-sea interaction model of intraseasonal oscillations in the tropics. *J. Atmos. Sci.*, **44**, 2324-2340 (1987).
14. Emanuel, K. A., J. D. Neelin, and C. S. Bretherton: On large-scale circulations in convecting atmospheres. *Quart. J. Roy. Meteor. Soc.*, **120**, 1111-1143 (1994).
15. Grabowski, W. W., Yano, J.-I., and Moncrieff, M. W.: Cloud-resolving modeling of tropical circulations driven by large-scale SST gradients. *J. Atmos. Sci.*, **57**, 2022-2039 (2000).
16. Gu, G., and C. Zhang: A spectrum analysis of synoptic-scale disturbances in the ITCZ. *J. Climate*, **14**, 2725-2739 (2001).
17. Gu G., Adler, R. F., and Sobel A. H.: The eastern Pacific ITCZ during the boreal spring. *J. Atmos. Sci.*, **62**, 1157-1174 (2005).
18. Holton, J. R., J. M. Wallace, and J. M. Young: On boundary layer dynamics and the ITCZ. *J. Atmos. Sci.*, **28**, 275-280 (1971)
19. Kleeman, R., : A simple model of the atmospheric response to ENSO sea surface temperature anomalies. *J. Atmos. Sci.*, **48**, 3-18 (1991).
20. Lin, J. W., J. D. Neelin, and N. Zeng: Maintenance of tropical intraseasonal variability: impact of evaporation-wind feedback and midlatitude storms. *J. Atmos. Sci.*, **57**, 2793-2823 (2000).
21. Lindzen, R. S., and S. Nigam: On the role of sea surface temperature gradients in forcing low-level winds and convergence in the tropics. *J. Atmos. Sci.*, **44**, 2418-2436 (1987).
22. Liu, W. T., and X. Xie: Double intertropical convergence zone-a new look using scatterometer. *Geophys. Res. Lett.*, **29**, 222072, doi:10.1029/2002GL015431 (2002).
23. Mapes, B. E.: Convective inhibition, subgridscale triggering, and stratiform instability in a toy tropical wave model. *J. Atmos. Sci.*, **57**, 1515-1535 (2000).
24. McGauley, M., C. Zhang, and N. A. Bond: Large-scale characteristics of the atmospheric boundary layer in the eastern Pacific cold tongue/ITCZ region. *J. Climate*, **17**, 3907-3920 (2004).
25. Moskowit B. M. and C. S. Bretherton: An Analysis of Frictional Feedback on a Moist Equatorial Kelvin Mode. *J. Atmos. Sci.*, **57**, 2188-2206 (2002).
26. Neelin, J. D.: On the interpretation of the Gill model. *J. Atmos. Sci.*, **46**, 2466-2468 (1989).
27. Neelin, J. D.: Implications of convective quasi-equilibria for the large-scale flow. *The physics and parameterization of moist atmospheric convection*, R. K. Smith, Ed., pp. 413-446, Elsevier (1997).
28. Neelin, J. D., and I. M. Held: Modeling tropical convergence based on the moist static energy budget. *Mon. Wea. Rev.*, **115**, 3-12 (1987)
29. Neelin, J. D., I. M. Held and K. H. Cook: Evaporation-wind feedback and low frequency variability in the tropical atmosphere. *J. Atmos. Sci.*, **44**, 2341-2348 (1987).

30. Neelin, J. D., and N. Zeng: A quasi-equilibrium tropical circulation model - formulation. *J. Atmos. Sci.*, **57**, 1741-1766 (2000).
31. Neelin, J. D., C. Chou, and H. Su: Tropical drought regions in global warming and El Niño teleconnections. *Geophys. Res. Lett.*, **30**(24), 2275, doi:10.1029/2003GL018625 (2003).
32. Neelin, J. D., and H. Su: Moist teleconnection mechanisms for the tropical South American and Atlantic sector. *J. Clim.*, **18**, 3928-3950 (2005).
33. Neggers, R., J. D. Neelin and B. Stevens: Impact mechanisms of shallow cumulus convection on tropical climate dynamics. *J. Clim.*, submitted (2005a).
34. Neggers, R., B. Stevens and J. D. Neelin: A simple equilibrium model for shallow cumulus convection. *Theoretical and Computational Fluid Dynamics*, submitted (2005b).
35. Nieto Ferreira, R., and W. H. Schubert: Barotropic aspects of ITCZ breakdown. *J. Atmos. Sci.*, **54**, 251-285 (1997).
36. Oort, A. H.: Global atmospheric circulation statistics, 1958-73. NOAA Professional Paper No. 14, U.S. Govt. Printing Office, Washington, DC, 180 pp plus 47 microfiches (1983).
37. Pauluis, O.: Boundary layer dynamics and cross-equatorial Hadley circulation. *J. Atmos. Sci.*, **61**, 1161-1173 (2004).
38. Pike, A. C.: The inter-tropical convergence zone studied with an interacting atmosphere and ocean model. *Mon. Wea. Rev.*, **99**, 469-477 (1971).
39. Raymond, D. J.: The thermodynamic control of tropical rainfall. *Quart. J. Royal Meteor. Soc.*, **564**, 889-898 (2000).
40. Raymond, D. J., Raga, G., Bretherton, C. S., Molinari, J., Lopez-Carillo, C., Fuchs, Z.: Convective forcing in the intertropical convergence zone of the eastern Pacific. *J. Atmos. Sci.*, **60**, 2064-2082 (2003).
41. Seager, R.: A simple model of the climatology and variability of the low-level wind field in the tropics. *J. Climate*, **4**, 164-179 (1991).
42. Shaevitz, D. A., and A. H. Sobel: Implementing the weak temperature gradient approximation with full vertical structure. *Mon. Wea. Rev.*, **132**, 662-669 (2004).
43. Sobel, A. H., and C. S. Bretherton: Modeling tropical precipitation in a single column. *J. Climate*, **13**, 4378-4392 (2000).
44. Stevens, B., J. Duan, J. C. McWilliams, M. Munnich, and J. D. Neelin: Entrainment, Rayleigh friction, and boundary layer winds over the tropical Pacific. *J. Climate*, **15**, 30-44 (2002).
45. Su, H., and J. D. Neelin: Teleconnection mechanisms for tropical Pacific descent anomalies during El Niño. *J. Atmos. Sci.*, **59**, 2694-2712 (2002).
46. Su, H. and J. D. Neelin: The scatter in tropical average precipitation anomalies. *J. Clim.*, **16**, 3966-3977 (2003).
47. Su, H., J. D. Neelin, and J. E. Meyerson: Mechanisms for lagged atmospheric response to ENSO SST forcing. *J. Clim.*, in press (2005).
48. Tomas, R. A., and P. J. Webster: The role of inertial instability in determining the location and strength of near-equatorial convection. *Q. J. R. Meteorol. Soc.*, **123**, 1445-1482 (1997)
49. Tomas, R. A., J. R. Holton, and P. J. Webster: The influence of cross-equatorial pressure gradients on the location of near-equatorial convection. *Q. J. R. Meteorol. Soc.*, **125**, 1107-1127 (1999).
50. Trenberth, K. E. and A. Solomon: The global heat balance: heat transports in the atmosphere and ocean. *Climate Dynamics*, **7**, 107-134 (1994).
51. Waliser, D. E., and R. C. J. Somerville: Preferred latitudes of the intertropical convergence zone. *J. Atmos. Sci.*, **51**, 1619-1639 (1994).
52. Wang, B., and T. Li: A simple tropical atmosphere model of relevance to short-term climate variations. *J. Atmos. Sci.*, **50**, 260-284 (1993)
53. Wang, C.-C., and G. Magnusdottir: ITCZ breakdown in three-dimensional flows. *J. Atmos. Sci.*, in press (2005).
54. Weare, B. C.: A simple model of the tropical atmosphere with circulation dependent heating and specific humidity. *J. Atmos. Sci.*, **43**, 2001-2016 (1986).
55. Webster, P. J.: Response of the tropical atmosphere to local, steady forcing. *Mon. Wea. Rev.*, **100**, 518-541 (1972).
56. Webster, P. J.: Mechanisms determining the atmospheric response to sea surface temperature anomalies. *J. Atmos. Sci.*, **38**, 554-571 (1980).
57. Wu, Z., Sarachik, E. S., Battisti, D. S.: Thermally forced surface winds on an equatorial beta plane. *J. Atmos. Sci.*, **56**, 2029-2037 (1999).
58. Wu, Z., Battisti, D. S., Sarachik, E. S.: Rayleigh friction, Newtonian cooling, and the linear response to steady tropical heating. *J. Atmos. Sci.* **57**, 1937-1957 (2000).
59. Yanai, M., Esbensen, S., Chu, J.-H.: Determination of bulk properties of tropical cloud clusters from large-scale heat and moisture budgets. *J. Atmos. Sci.*, **30**, 611-627 (1973).
60. Yu, J.-Y., and J. D. Neelin: Analytic approximations for moist convectively adjusted regions. *J. Atmos. Sci.*, **54**, 1054-1063 (1997).
61. Yu, J.-Y., C. Chou, and J. D. Neelin: Estimating the gross moist stability of the tropical atmosphere. *J. Atmos. Sci.*, **55**, 1354-1372 (1998).
62. Zebiak, S. E.: A simple atmospheric model of relevance to El Niño. *J. Atmos. Sci.*, **39**, 2017-2027 (1982).
63. Zebiak, S. E.: Atmospheric convergence feedback in a simple model for El Niño. *Mon. Wea. Rev.*, **114**, 1263-1271 (1986).
64. Zeng, N., J. D. Neelin, and C. Chou: A quasi-equilibrium tropical circulation model - implementation and simulation. *J. Atmos. Sci.*, **57**, 1767-1796 (2000).

65. Zeng, N., and J. D. Neelin: A land-atmosphere interaction theory for the tropical deforestation problem. *J. Clim.*, **12**, 857-872 (1999).
66. Zhang, C., M. McGauley, and N. A. Bond: Shallow meridional circulation in the tropical eastern Pacific. *J. Climate*, **17**, 133-139 (2004).